

P-05-96

Oskarshamn site investigation

Borehole KLX03A

Triaxial compression test of intact rock

Lars Jacobsson
SP Swedish National Testing and Research Institute

June 2005

Svensk Kärnbränslehantering AB

Swedish Nuclear Fuel
and Waste Management Co
Box 5864

SE-102 40 Stockholm Sweden

Tel 08-459 84 00

+46 8 459 84 00

Fax 08-661 57 19

+46 8 661 57 19



Oskarshamn site investigation

Borehole KLX03A

Triaxial compression test of intact rock

Lars Jacobsson

SP Swedish National Testing and Research Institute

June 2005

Keywords: Rock mechanics, Triaxial compression test, Elasticity parameters, Stress-strain curve, Post-failure behaviour.

This report concerns a study which was conducted for SKB. The conclusions and viewpoints presented in the report are those of the author and do not necessarily coincide with those of the client.

A pdf version of this document can be downloaded from www.skb.se

Abstract

Triaxial compression tests with constant confining pressure, containing the complete loading response beyond compressive failure, so called post-failure tests, were carried out on 12 water saturated specimens of intact rock from borehole KLX03A in Laxemar. The cylindrical specimens were taken from rock cores at three depth levels ranging between 294–314 m, 513–515 m and 693–695 m. Moreover, the rock types were mapped as Ävrö granite (294–314 m and 513–515 m) and Quartz monzodiorite (693–695 m). The elastic properties, represented by the Young's modulus and the Poisson ratio, and the compressive strength were deduced from these tests. The wet density of the specimens was determined before the mechanical tests. The specimens were documented by photographing the specimens before and after the mechanical testing.

The measured densities for the water saturated specimens were in the range 2,760–2,820 kg/m³, which yield a mean value of 2,787 kg/m³. Three confining pressure levels were used, 2, 7 and 15 MPa, and the peak values of the axial compressive stress were in the range 178.2–303.5 MPa. The elastic parameters were determined at load corresponding to 50% of the failure load and it was found that Young's modulus was in the range 59.4–79.0 GPa with a mean value of 68.9 GPa and the Poisson ratio was in the range of 0.17–0.24 with a mean value of 0.21. It was seen from the mechanical tests that the material in the specimens responded in a brittle way.

Sammanfattning

Triaxiella kompressionsprov med belastning upp till brott och efter brott, så kallade ”post-failure tests”, har genomförts på 12 stycken vattenmättade cylindriska provobjekt av intakt berg. Provobjekten har tagits från en borrhärla från borrhål KLX03A i Laxemar vid tre djupnivåer 294–314 m, 513–515 m och 693–695 m. Bergtyperna vid dessa nivåer var Ävrö granit (294–314 m och 513–515 m) och Kvartsmonzodiorite (693–695 m). De elastiska egenskaperna, representerade av elasticitetsmodulen och Poissons tal, har bestämts ur försöken. Bergmaterialets densitet i vått tillstånd hos proverna mättes upp före de mekaniska proven. Provobjekten fotograferades före och efter de mekaniska proven.

Den uppmätta densiteten hos de vattenmättade proven var mellan 2 760–2 820 kg/m³ med ett medelvärde på 2 787 kg/m³. Tre olika celltryck användes vid triaxialproven 2, 7 och 15 MPa och toppvärdena för den axiella kompressiva spänningen låg mellan 178,2–303,5 MPa. De elastiska parametrarna bestämdes vid en last motsvarande 50% av topplasten vilket gav en elasticitetsmodul mellan 59,4–79,0 GPa med ett medelvärde på 68,9 GPa och Poissons tal mellan 0,17–0,24 med ett medelvärde på 0,21. Vid belastningsförsöken kunde man se att materialet i provobjekten hade ett sprött beteende.

Contents

1	Introduction	7
2	Objective and scope	9
3	Equipment	11
3.1	Specimen preparation and density measurement	11
3.2	Mechanical testing	11
4	Execution	13
4.1	Description of the specimens	13
4.2	Specimen preparation and density measurement	13
4.3	Mechanical testing	14
4.4	Data handling	15
4.5	Analyses and interpretation	15
5	Results	17
5.1	Description and presentation of the specimen	17
5.2	Results for the entire test series	42
5.3	Discussion	42
	References	45
	Appendix A	47
	Appendix B	49

1 Introduction

Triaxial compression tests, with loading beyond the failure point into the post-failure regime, have been conducted on water-saturated specimens sampled from borehole KLX03A in Laxemar, see map in Figure 1-1. These tests belong to one of the activities performed as part of the site investigation in the Oskarshamn area conducted by the Swedish Nuclear Fuel and Waste Management Co (SKB). The tests were carried out in the material and rock mechanics laboratories at the department of Building Technology and Mechanics at the Swedish National Testing and Research Institute (SP). All work is carried out in accordance with the activity plan AP PS 400-04-106 (SKB internal controlling document) and is controlled by SP-QD 13.1 (SP internal quality document).

SKB supplied SP with rock cores and they arrived at SP in December 2004 and were tested during April 2004. Cylindrical specimens were cut from the cores and selected based on the preliminary core logging with the strategy to primarily investigate the properties of the dominant rock type. The method description SKB MD 190.003, version 2.0 (SKB internal controlling document) was followed both for the sampling and for the triaxial compression tests and the method description SKB MD 160.002, version 2.0 (SKB internal controlling document) was followed when the density was determined. As to the specimen preparation, the end surfaces on the specimens were grinded in order to comply with the required shape tolerances and kept stored in water, with a minimum of 7 days, up to testing. This yields a water saturation, which is intended to resemble the in-situ moisture condition. The density was determined on each specimen and the triaxial compression tests were carried out at this moisture condition at different confining pressures. The specimens were photographed before and after the mechanical testing.

The triaxial compression tests were carried out using radial strain as the feed back signal in order to obtain the complete response in the post-failure regime on brittle specimens as is described in the method description SKB MD 190.003, version 2.0 (SKB internal controlling document) and in the ISRM suggested method /1/. The axial ϵ_a and radial strain ϵ_r together with the axial stress σ_a were recorded during the test. The peak value of the axial compressive stress σ_c was determined at each test. Furthermore, two elasticity parameters, Young's modulus E and Poisson ratio ν , were deduced from the tangent properties at 50% of the peak load. Diagrams with the volumetric and crack volumetric strain versus axial stress are reported. These diagrams can be used to determine crack initiation stress σ_i and the crack damage stress σ_d , cf /2, 3/.

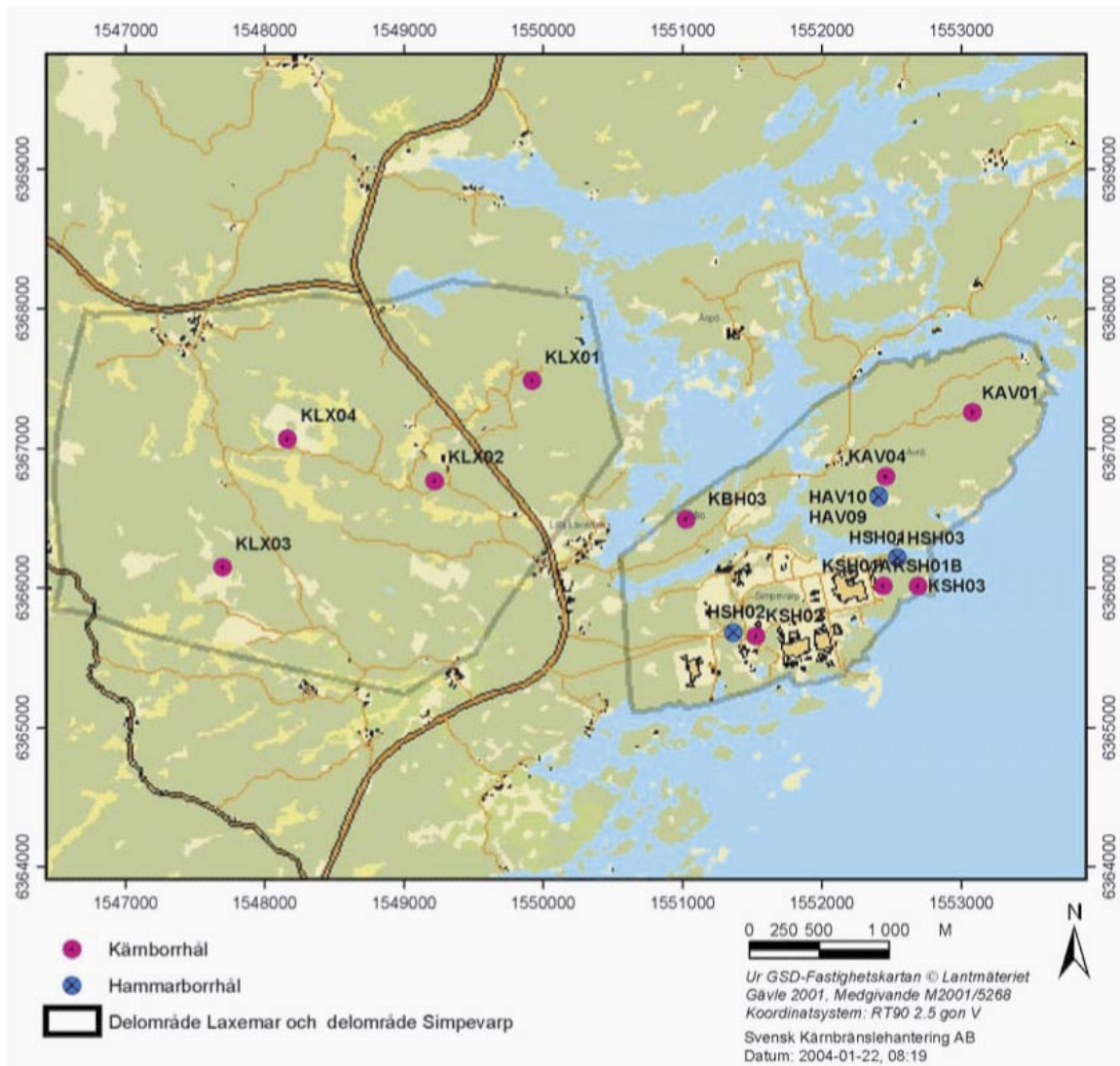


Figure 1-1. Location of the borehole KLX03A at the Laxemar site.

2 Objective and scope

The purpose of the testing is to determine the compressive strength and the elastic properties, represented by the Young's modulus and the Poisson ratio, of confined cylindrical intact rock specimens at different confining pressures. Moreover, the specimens are sampled from drill cores and have a water content corresponding to the in-situ conditions. The loading is carried out into the post-failure regime in order to study the mechanical behaviour of the rock after cracking and thereby be able to determine the brittleness and residual strength. The specimens are from the borehole KLX03A, which has a drilling depth of c 1,000 m.

The results from the tests are going to be used in the site descriptive rock mechanics model, which will be established for the candidate area selected for site investigations at Oskarshamn.

3 Equipment

3.1 Specimen preparation and density measurement

A circular saw with a diamond blade was used to cut the specimens to their final lengths. The surfaces were then grinded after cutting in a grinding machine in order to achieve a high-quality surface for the axial loading that complies with the required tolerances. The measurements of the specimen dimensions were made with a sliding calliper. Furthermore, the tolerances were checked by means of a dial indicator and a stone face plate. The specimen preparation is carried out in accordance with ASTM 4543-01 /4/.

The specimens and the water were weighed using a scale weighing machine. A thermometer was used for the water temperature measurement. The calculated wet density was determined with an uncertainty of $\pm 4 \text{ kg/m}^3$.

3.2 Mechanical testing

The mechanical tests were carried out in servo controlled testing machine specially designed for rock tests, see Figure 3-1. The system contains of a load frame, a hydraulic pump unit, a controller unit and various sensors. The communication with the controller unit is accomplished by means of special testing software running on a PC that is connected to the controller. The load frame has a high stiffness and a fast responding actuator, cf the ISRM suggested method /1/. Furthermore, the sensors, the controller and the servo valve are fast responding components. The machine is equipped with a pressure vessel in which the specimens are tested under a confinement pressure. A thin rubber membrane is mounted on the specimen in order to seal the specimen from the oil used that is used as the confinement medium, cf Figure 3-2. The axial load is determined using a load cell, which is located inside the pressure vessel and has a maximum capacity of 1.5 MN. The uncertainty of the load measurement is less than 1%.

The axial and circumferential (radial) deformation of the rock specimen was measured. The rock deformation measurement systems are based on miniature LVDTs, which has a measurement range of $\pm 2.5 \text{ mm}$. The LVDTs were calibrated by means of a micrometer and they displayed an accuracy of $\pm 2.5\%$ within a $\pm 2 \text{ mm}$ range that was used in the tests. The axial deformation measurement system comprises two aluminium rings that are attached on the specimen placed approximately at $\frac{1}{4}$ and $\frac{3}{4}$ of the specimen height, cf Figures 3-2 and 4-1. Two LVDTs mounted on the rings are used to measure the distance change between the rings on opposite side of the specimen. The rings have three adjustable spring-loaded screws each with a rounded tip pointing towards the specimen with 120 degrees division. The rings are mounted directly on the rubber membrane. The pre-load of the screws fixates the rings. The position of the frame piston was also stored during the test in order to give a possibility for comparison with the measurements made with the measurement system that was based on the rings displacement.

The radial deformation was obtained by using a chain mounted around the specimen at mid-height, see Figure 3-2. The change of the chain-opening gap was measured by means of one LVDT and the circumferential and thereby also the radial deformation could be obtained. See Appendix A.

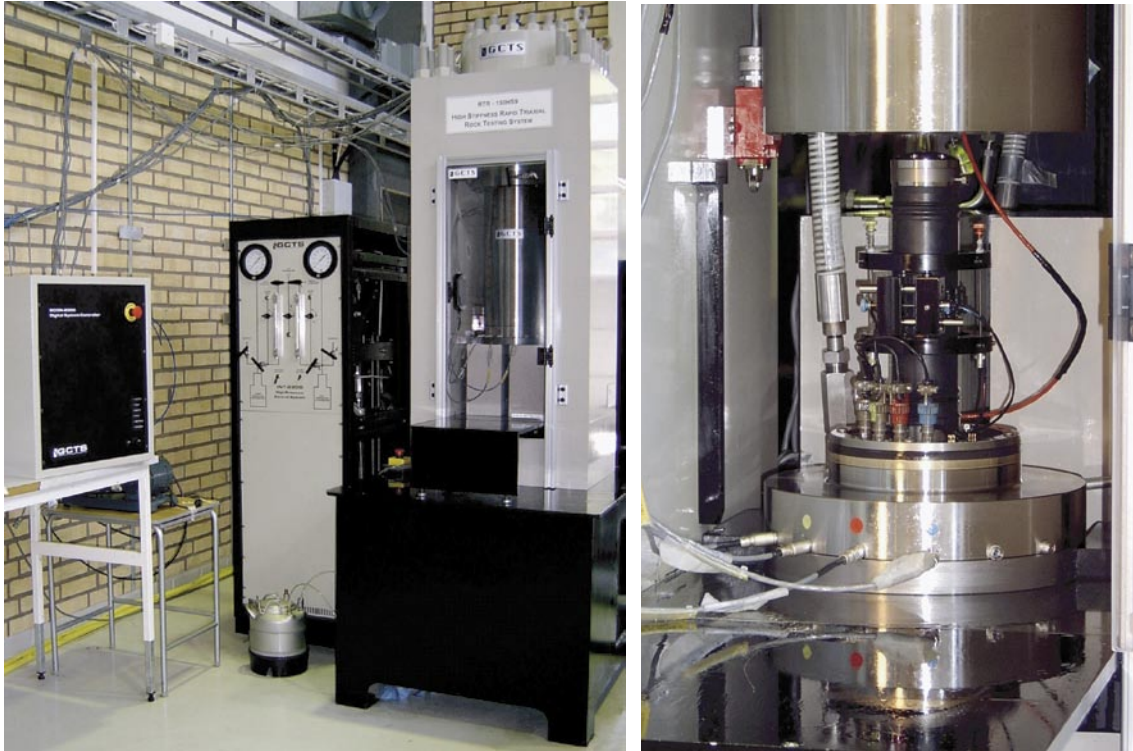


Figure 3-1. Left: Digital controller unit, pressure cabinet with cell pressure intensifier and oil reservoir inside, load frame with closed cell (pressure vessel). Right: Bottom of the cell is lowered. The specimen is instrumented and ready for inserting in the cell.

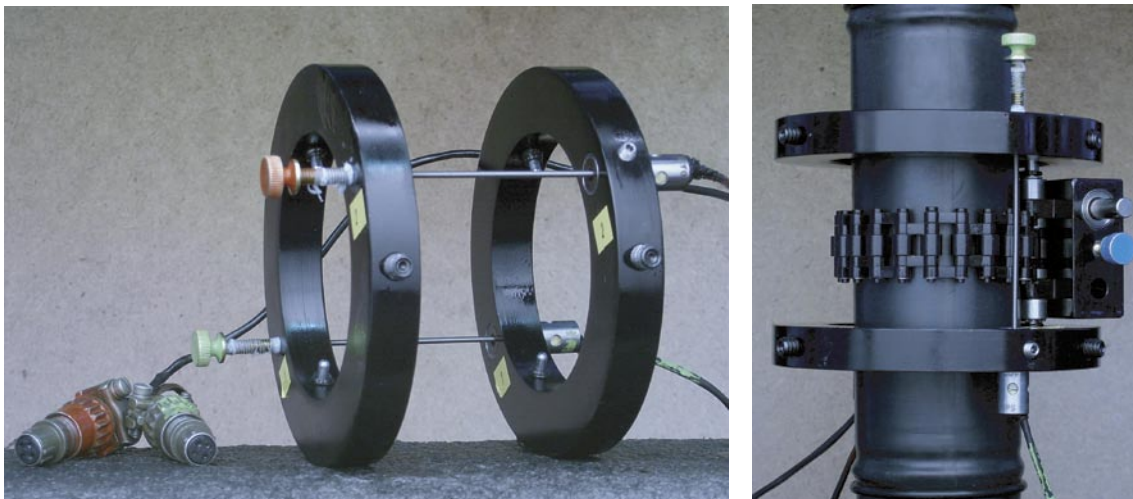


Figure 3-2. Left: Rings and LVDTs for axial deformation measurement. Right: Specimen and loading platens sealed with a rubber membrane. Devices for axial and circumferential deformation measurements are attached.

The specimens were photographed with a 4.0 Mega pixel digital camera at highest resolution and the photographs were stored in a jpeg-format.

4 Execution

The water saturation and determination of the density of the wet specimens were made in accordance with the method description SKB MD 160.002, version 2.0 (SKB internal controlling document). This includes determination of density in accordance to ISRM /5/ and water saturation by SS EN 13755 /6/. The triaxial compression tests were carried out according to the method description SKB MD 190.003, version 2.0 (SKB internal controlling document). The test method is based on the ISRM suggested methods /1/ and /7/.

4.1 Description of the specimens

The rock type characterisation was made according to Strähle /8/ using the SKB mapping system (Boremap). The identification marks, upper and lower sampling depth (Secup and Seclow) and the rock type are shown in Table 4-1.

Table 4-1. Specimen identification, sampling depth, confining pressure at the triaxial tests and rock type for all specimens (based on the overview mapping).

Identification	Secup (m)	Seclow (m)	Confining pressure (MPa)	Rock type
KLX03A-115-1	294.03	294.17	2	Ävrö granite
KLX03A-115-3	294.54	294.68	7	Ävrö granite
KLX03A-115-4	313.50	313.64	15	Ävrö granite
KLX03A-115-5	313.64	313.78	7	Ävrö granite
KLX03A-115-6	513.79	513.93	2	Ävrö granite
KLX03A-115-7	513.93	514.05	7	Ävrö granite
KLX03A-115-8	514.07	514.21	7	Ävrö granite
KLX03A-115-9	514.21	514.35	15	Ävrö granite
KLX03A-115-11	693.86	694.00	2	Quartz monzodiorite
KLX03A-115-12	694.00	694.14	7	Quartz monzodiorite
KLX03A-115-13	694.14	694.28	7	Quartz monzodiorite
KLX03A-115-14	694.68	694.82	15	Quartz monzodiorite

4.2 Specimen preparation and density measurement

The temperature of the water was 18.0°C, which equals to a water density of 998.6 kg/m³, when the determination of the wet density of the rock specimens was carried out. Further, the specimens had been stored 14 days in water when the density was determined.

An overview of the activities during the specimen preparation is shown in the step-by step description in Table 4-2.

Table 4-2. Activities during the specimen preparation.

Step	Activity
1	The drill cores were marked where the specimens are to be taken.
2	The specimens were cut to the specified length according to markings and the cutting surfaces were grinded.
3	The tolerances were checked: parallel and perpendicular end surfaces, smooth and straight circumferential surface.
4	The diameter and height were measured three times each. The respectively mean value determines the dimensions that are reported.
5	The specimens were then water saturated according to the method described in SKB MD 160.002, version 2.0 (SKB internal controlling document) and were stored for minimum 7 days in water whereupon the wet density was determined.

4.3 Mechanical testing

The specimens had been stored 24–30 days in water when the triaxial compression tests were carried out. The functionality of the triaxial testing system was checked, by carrying out tests on other cores with a similar type rock before the tests described in this report started. A check-list was filled in successively during the work in order to confirm that the different specified steps had been carried out. Moreover, comments were made upon observed things during the mechanical testing that are relevant for the interpretation of the results. The check-list form is a SP internal quality document.

An overview of the activities during the mechanical testing is shown in the step-by step description in Table 4-3.

Table 4-3. Activities during the mechanical testing.

Step	Activity
1	Digital photos were taken on each specimen before the mechanical testing.
2	The specimen was put in testing position and centred between the loading platens.
3	A rubber membrane was mounted on the specimen and the devices for measuring axial and circumferential deformations were attached to the specimen on top of the rubber membrane.
4	The core on each LVDT was adjusted by means of a set screw to the right initial position. This was done so that the optimal range of the LVDTs can be used for the deformation measurement.
5	The triaxial cell was closed and filled with oil whereby a cell pressure of 0.6 MPa is applied.
6	The frame piston was brought down into contact with the specimen with a force corresponding to a deviatoric stress of 0.6 MPa. The cell pressure was then raised to the specified level and at the same time keeping the deviatoric stress constant.
7	The deformation measurement channels were zeroed in the test software.
8	The loading was started and the initial loading rate was set to a radial strain rate of $-0.025\%/min$. The loading rate was increased after reaching the post-failure region. This was done in order to prevent the total time for the test to become too long.
9	The test was stopped either manually when the test had proceeded large enough to reveal the post-failure behaviour, or after severe cracking had occurred and it was judged that very little residual axial loading capacity was left in the specimen.
10	The oil pressure was brought down to zero and the oil was poured out of the cell. The cell was opened and the specimen taken out.
11	Digital photos were taken on each specimen after the mechanical testing.

4.4 Data handling

The test results were exported as text files from the test software and stored in a file server on the SP computer network after each completed test. The main data processing, in which the elastic moduli were computed and the peak stress was determined, has been carried out in the program MATLAB /9/. Moreover, MATLAB was used to produce the diagrams shown in section 5.1 and in Appendix B. The summary of results in section 5.2 with tables containing mean value and standard deviation of the different parameters and diagrams were produced using MS Excel. MS Excel was also used for reporting data to the SICADA database.

4.5 Analyses and interpretation

As to the definition of the different results parameters we begin with the axial stress σ_a , which is defined as

$$\sigma_a = \frac{F}{A}$$

where F is the axial force acting on the specimen and A is specimen cross section area. The pressure vessel (triaxial cell) filled with oil specimen is pressurized with a cell (confining) pressure p . This implies that the specimen becomes confined and the radial stress σ_r of the specimen is equal to confining pressure p . The (effective) deviatoric stress is defined as

$$\tilde{A}_{\text{dev}} = \tilde{A}_a - \tilde{A}_r$$

The peak value of the axial stress during a test is representing the triaxial compressive strength σ_c , for the actual confining pressure used in the test, in the results presentation.

The average value of the two axial displacement measurements on opposite sides of the specimen is used for the axial strain calculation. The recorded deformation δ_{local} represents a local axial displacement between the points approximately at $\frac{1}{4}$ and $\frac{3}{4}$ of the specimen height, cf Figure 4-1. The axial strain is defined as

$$\varepsilon_a = \delta_{\text{local}} / L_{\text{local}}$$

where L_{local} is the distance between the rings before loading.

The radial deformation is measured by means of a chain mounted around the specimen at mid-height, see Figure 3-2. The change of chain opening gap is measured by means of one LVDT. This measurement is used to compute the radial strain ε_r , see Appendix A. Moreover, the volumetric strain ε_{vol} is defined as

$$\varepsilon_{\text{vol}} = \varepsilon_a + 2\varepsilon_r$$

The stresses and the strains are defined as positive in compressive loading and deformation. The elasticity parameters are defined by the tangent Young's modulus E and tangent Poisson ratio ν as

$$E = \frac{\sigma_a(0.60\sigma_c) - \sigma_a(0.40\sigma_c)}{\varepsilon_a(0.60\sigma_c) - \varepsilon_a(0.40\sigma_c)}$$

$$\nu = -\frac{\varepsilon_r(0.60\sigma_c) - \varepsilon_r(0.40\sigma_c)}{\varepsilon_a(0.60\sigma_c) - \varepsilon_a(0.40\sigma_c)}$$

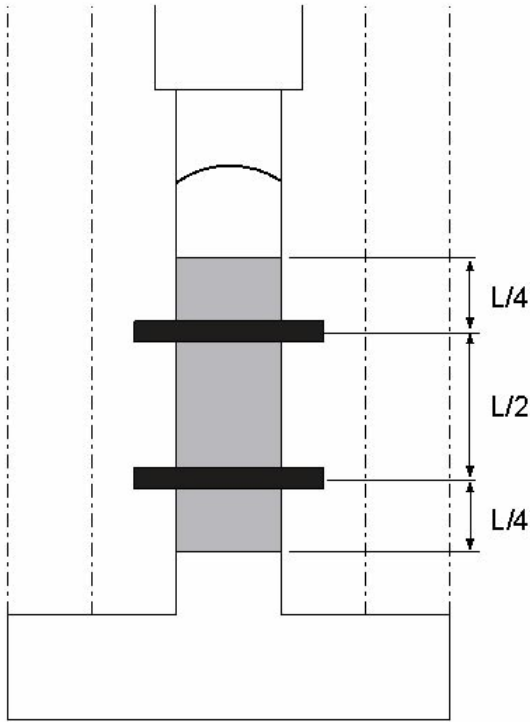


Figure 4-1. Sketch showing the triaxial cell with the rock specimen (grey) with height L and the placement of the rings (black) used for the axial deformation measurements. The membrane is omitted in the figure for simplicity.

The tangents were evaluated with values corresponding to an axial load between 40% and 60% of the axial peak stress σ_c .

A closure of present micro cracks will take place initially during confinement and axial loading. Development of new micro cracks will start when the axial load is further increased and axial stress reaches the crack initiation stress σ_i . The crack growth at this stage is as stable as increased loading is required for further cracking. A transition from a development of micro cracks to macro cracks will take place when the axial load is further increased. At a certain stress level the crack growth becomes unstable. The stress level when this happens is denoted the crack damage stress σ_d , cf /2, 3/. In order to determine the stress levels we look at the volumetric strain.

By subtracting the elastic volumetric strain ϵ_{vol}^e from the total volumetric strain a volumetric strain corresponding to the crack volume is obtained ϵ_{vol}^{cr} . This has been denoted calculated crack volumetric strain in the literature, cf /2, 3/. We have thus

$$\epsilon_{vol}^{cr} = \epsilon_{vol} - \epsilon_{vol}^e$$

Assuming linear elasticity leads to

$$\epsilon_{vol}^{cr} = \epsilon_{vol} - \frac{1-2\nu}{E}(\sigma_a - \sigma_r)$$

Experimental investigations have shown that the crack initiation stress σ_i coincides with the onset of increase of the calculated crack volume, cf /2, 3/. The same investigations also indicate that the crack damage stress σ_d can be defined as the axial stress at which the total volume starts to increase, i.e. when a dilatant behaviour is observed.

5 Results

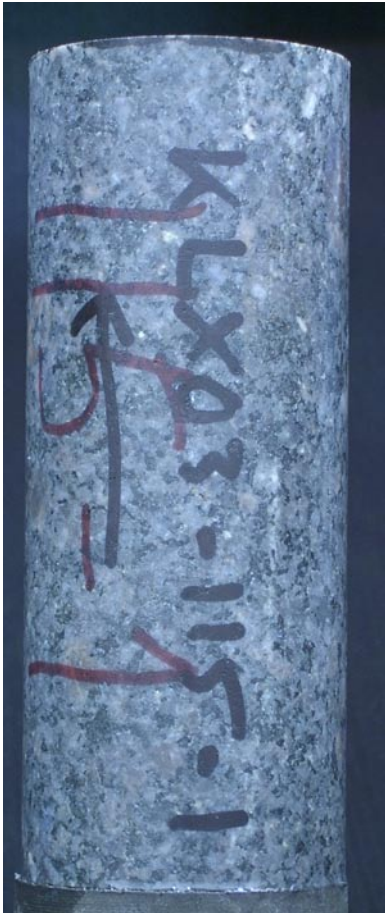
The results of the individual specimens are presented in section 5.1 and a summary of the results is given in section 5.2. The reported parameters are based on unprocessed raw data obtained from the testing and were reported to the SICADA database. These data together with the digital photographs of the individual specimens were handed over to SKB. The handling of the results follows SDP-508 (SKB internal controlling document) in general.

5.1 Description and presentation of the specimen

The cracking is shown in pictures taken on the specimens with comments on observed things that appeared during the testing. The elasticity parameters have been evaluated by using the results from the local deformation measurements. Red rings are superposed on the graphs indicating every five minutes of the progress of testing. The results for the individual specimens are as follows:

Specimen ID: KLX03A-115-1

Before mechanical test



After mechanical test

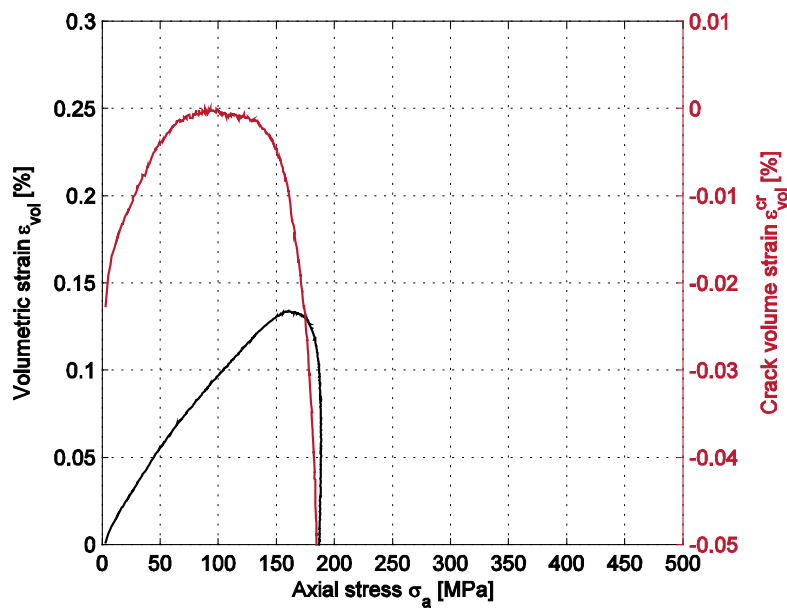
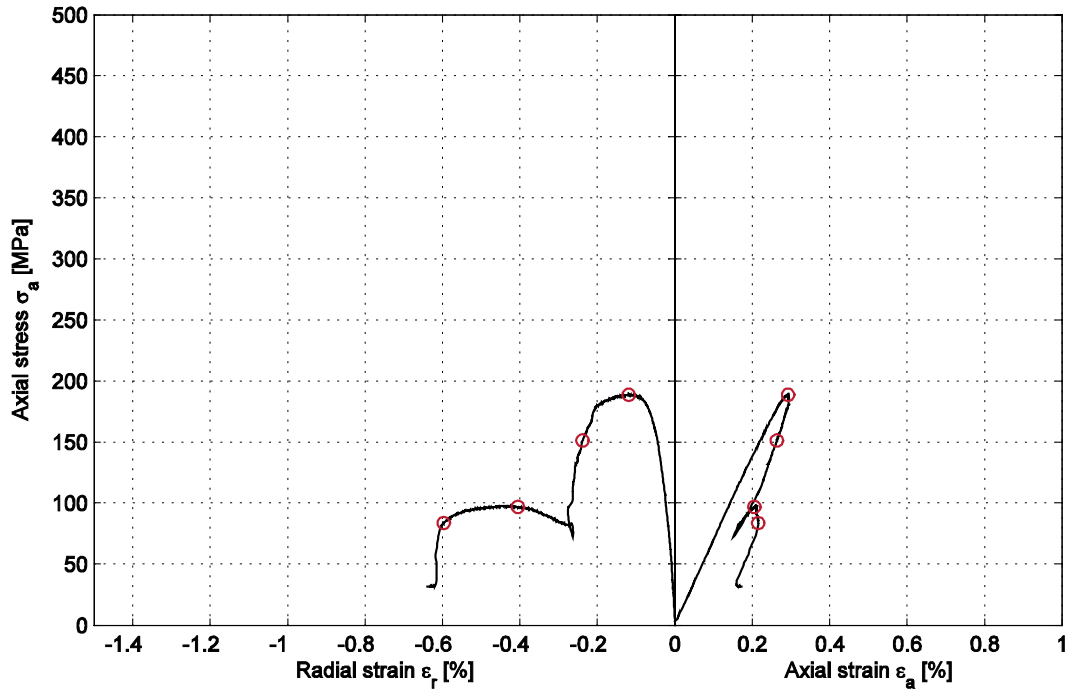


Diameter (mm)	Height (mm)	Density (kg/m³)
50.2	127.5	2,770

Comments Diagonal shear failure.

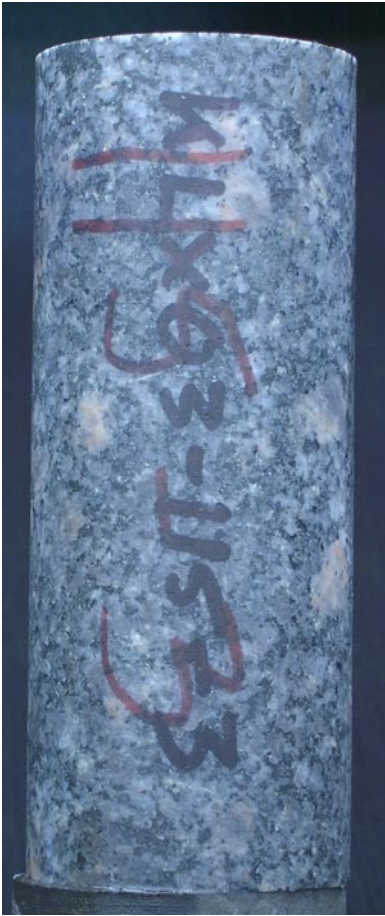
Specimen ID: KLX03A-115-01

Youngs Modulus (E): 69.9 [GPa] Cell pressure: 2 [MPa]
Poisson Ratio (ν): 0.234 [-]
Axial peak stress (σ_c): 188.7 [MPa]



Specimen ID: KLX03A-115-3

Before mechanical test



After mechanical test



Diameter (mm)	Height (mm)	Density (kg/m³)
50.2	127.7	2,770

Comments V-shaped shear failure.

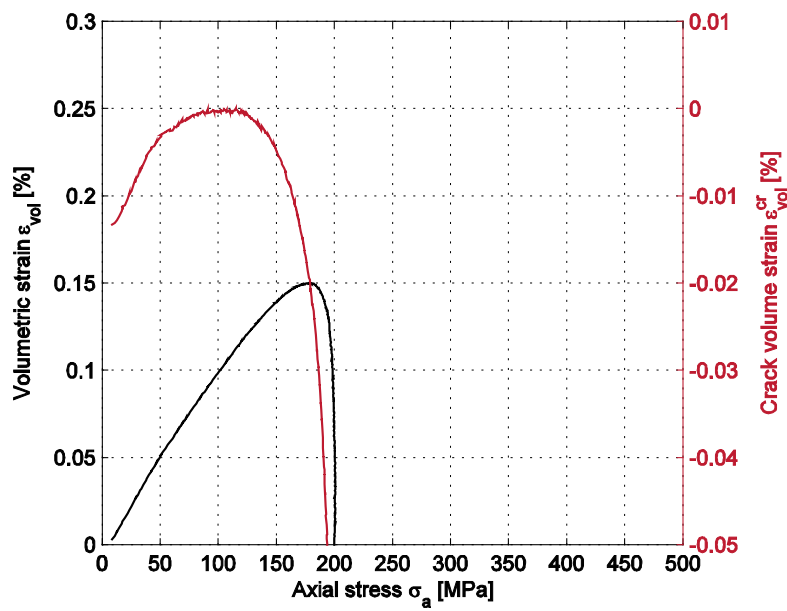
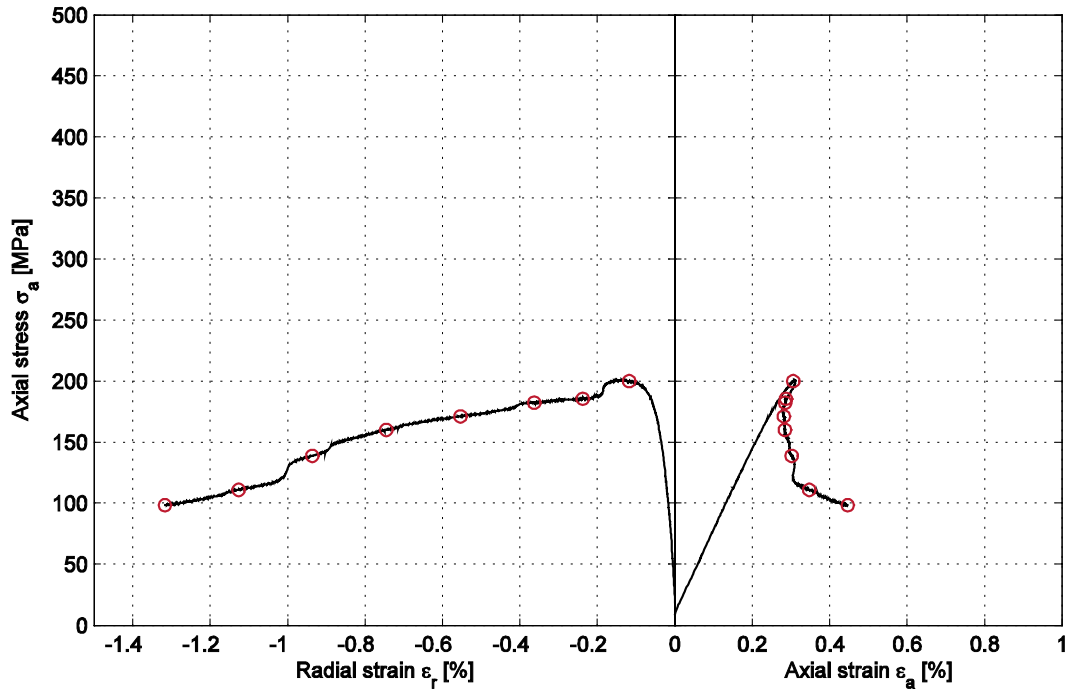
Specimen ID: KLX03A-115-03

Youngs Modulus (E): 67 [GPa]

Cell pressure: 7 [MPa]

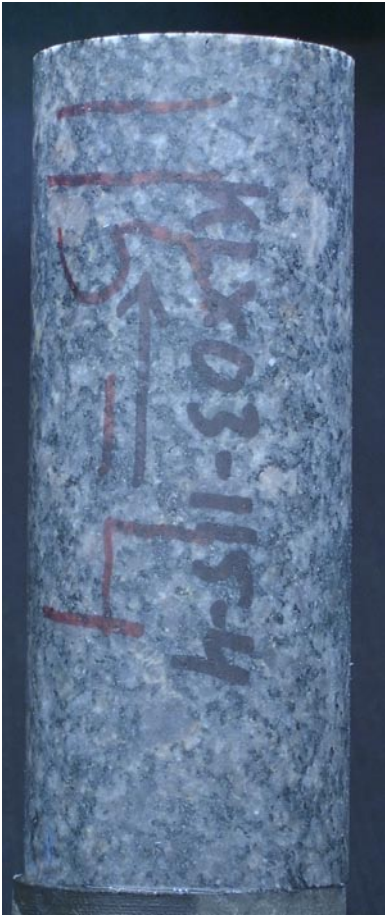
Poisson Ratio (ν): 0.198 [-]

Axial peak stress (σ_c): 200.9 [MPa]



Specimen ID: KLX03A-115-4

Before mechanical test



After mechanical test



Diameter (mm)	Height (mm)	Density (kg/m³)
50.2	127.8	2,780

Comments V-shaped shear failure.

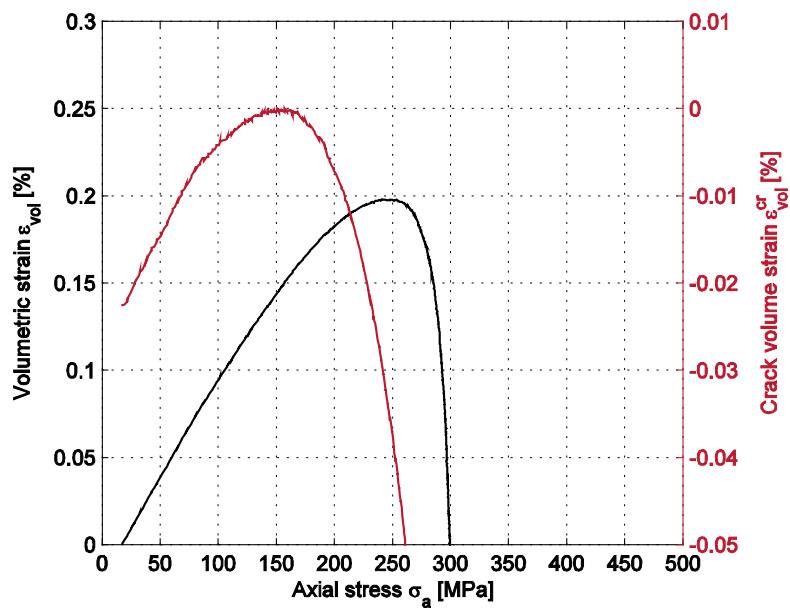
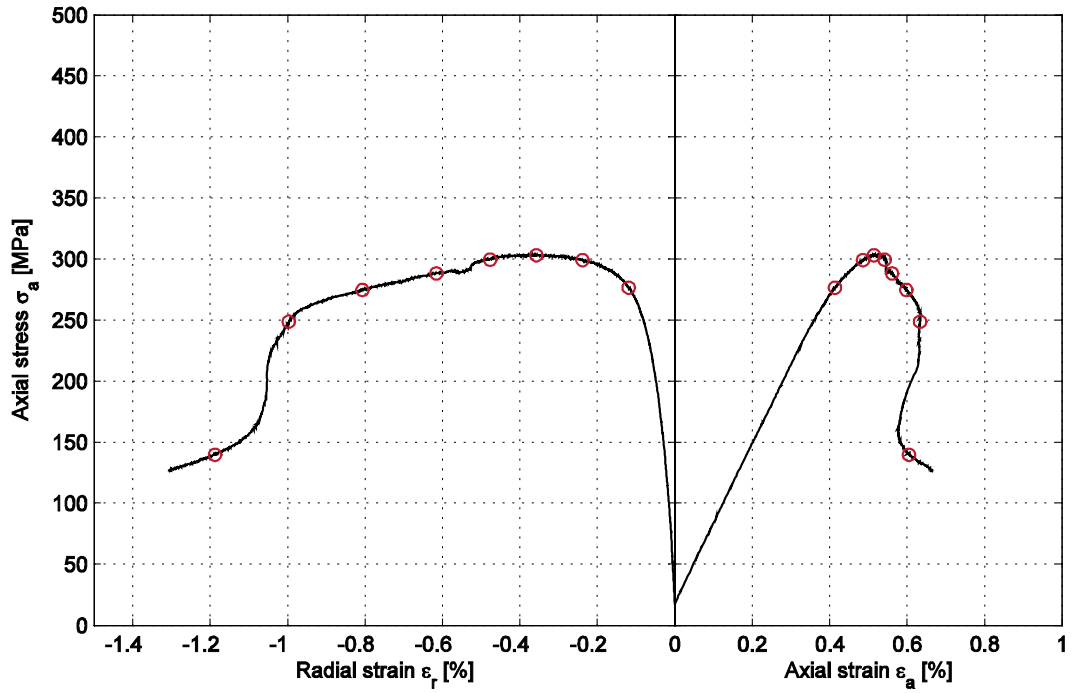
Specimen ID: KLX03A-115-04

Youngs Modulus (E): 64.1 [GPa]

Cell pressure: 15 [MPa]

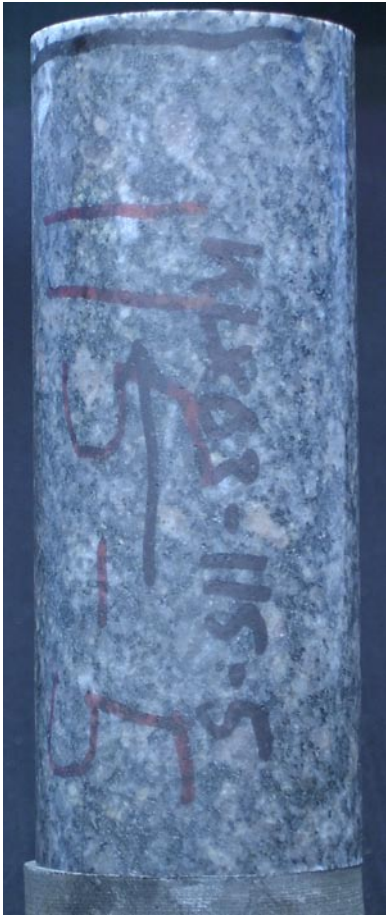
Poisson Ratio (ν): 0.208 [-]

Axial peak stress (σ_c): 303.5 [MPa]



Specimen ID: KLX03A-115-5

Before mechanical test



After mechanical test



Diameter (mm)	Height (mm)	Density (kg/m³)
50.2	127.5	2,770

Comments V-shaped shear failure.

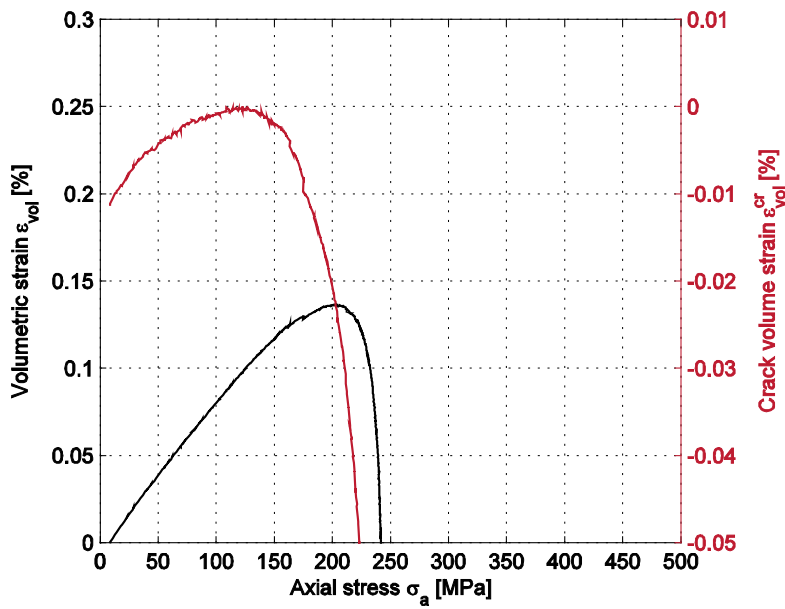
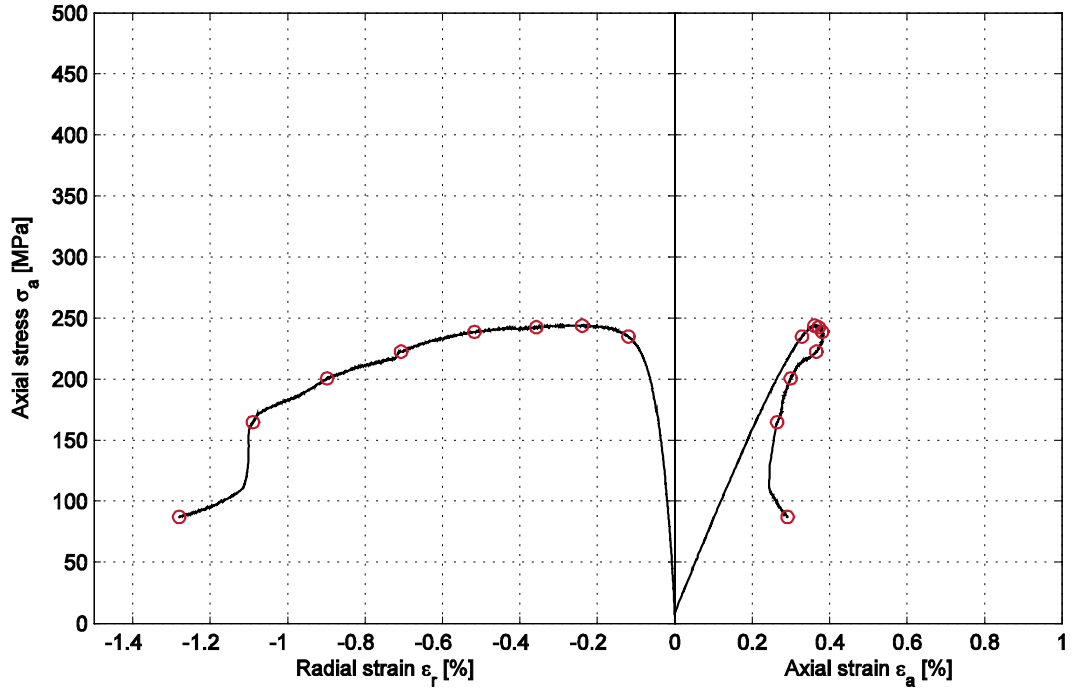
Specimen ID: KLX03A-115-05

Youngs Modulus (E): 73 [GPa]

Cell pressure: 7 [MPa]

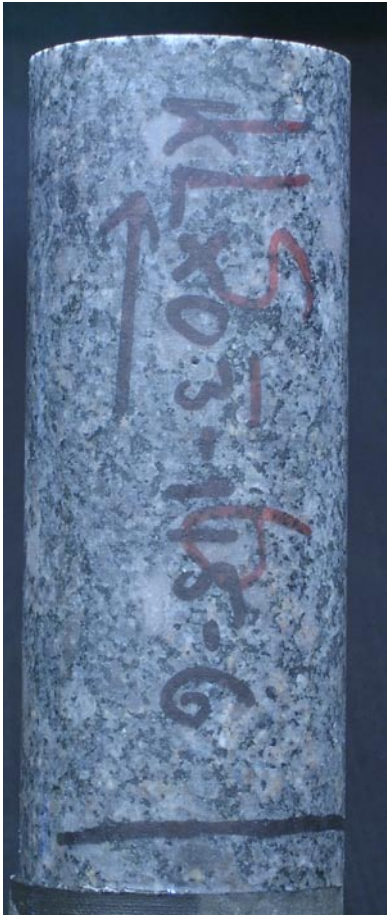
Poisson Ratio (ν): 0.223 [-]

Axial peak stress (σ_c): 244 [MPa]



Specimen ID: KLX03A-115-6

Before mechanical test



After mechanical test



Diameter (mm)	Height (mm)	Density (kg/m³)
50.2	127.5	2,760

Comments V-shaped shear failure.

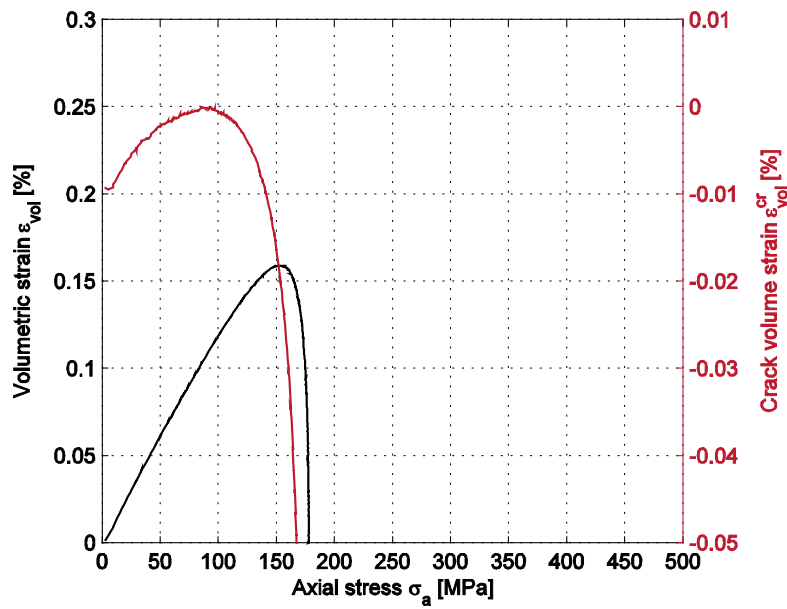
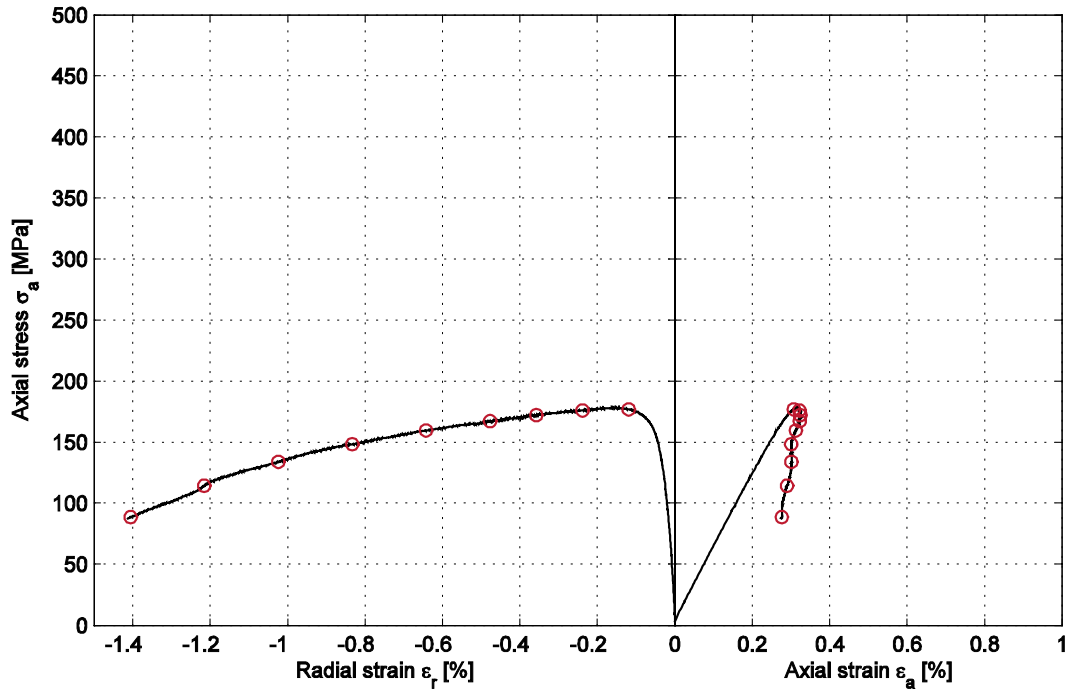
Specimen ID: KLX03A-115-06

Youngs Modulus (E): 59.4 [GPa]

Cell pressure: 2 [MPa]

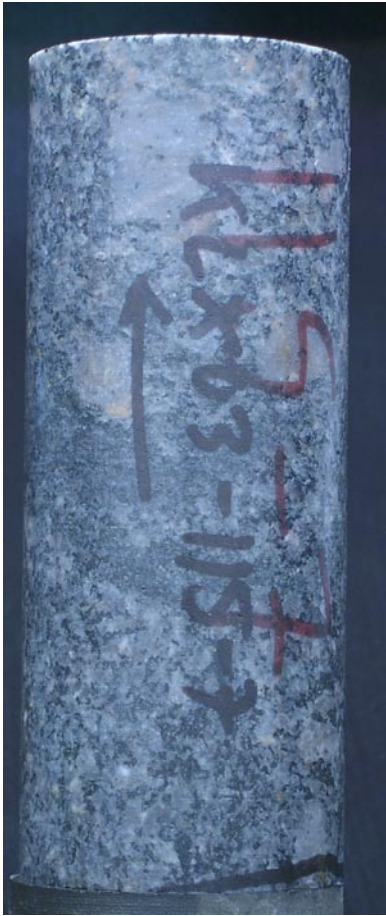
Poisson Ratio (ν): 0.169 [-]

Axial peak stress (σ_c): 178.2 [MPa]



Specimen ID: KLX03A-115-7

Before mechanical test



After mechanical test



Diameter (mm)	Height (mm)	Density (kg/m³)
50.2	127.5	2,780

Comments Diagonal shear failure.

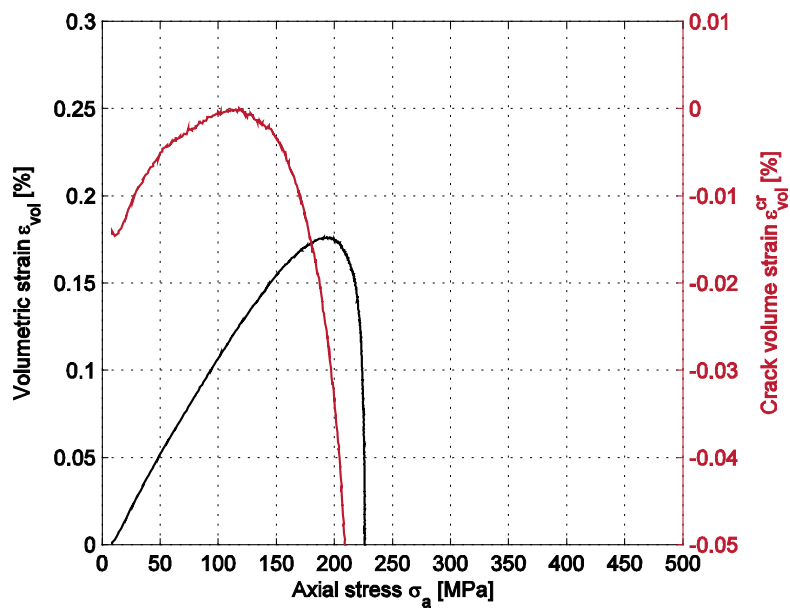
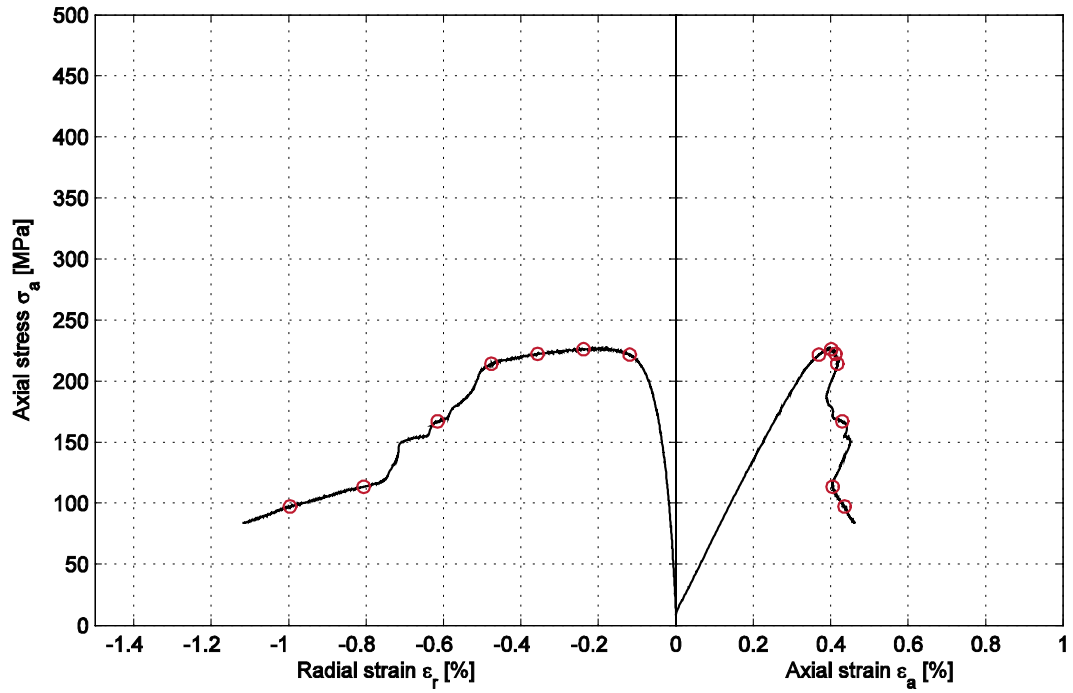
Specimen ID: KLX03A-115-07

Youngs Modulus (E): 61.4 [GPa]

Cell pressure: 7 [MPa]

Poisson Ratio (ν): 0.19 [-]

Axial peak stress (σ_c): 226.5 [MPa]



Specimen ID: KLX03A-115-8

Before mechanical test



After mechanical test



Diameter (mm)	Height (mm)	Density (kg/m³)
50.2	125.1	2,780

Comments Diagonal shear failure.

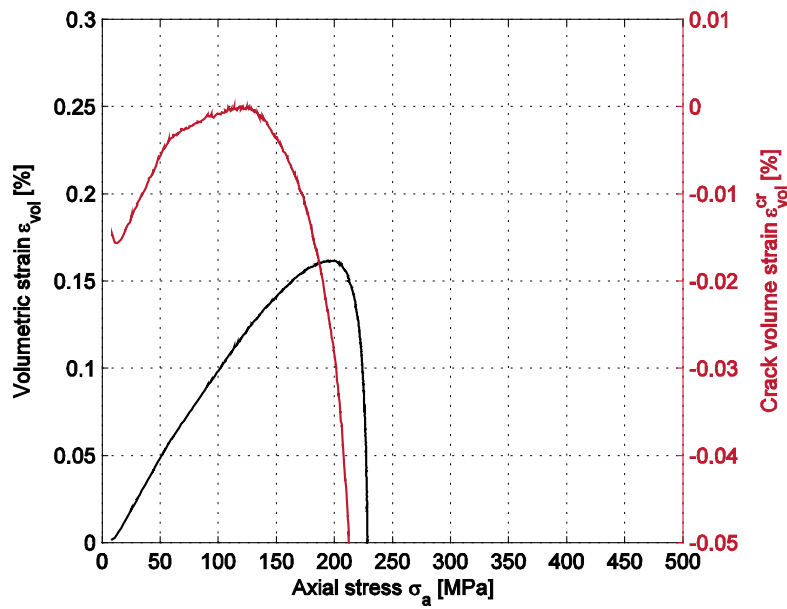
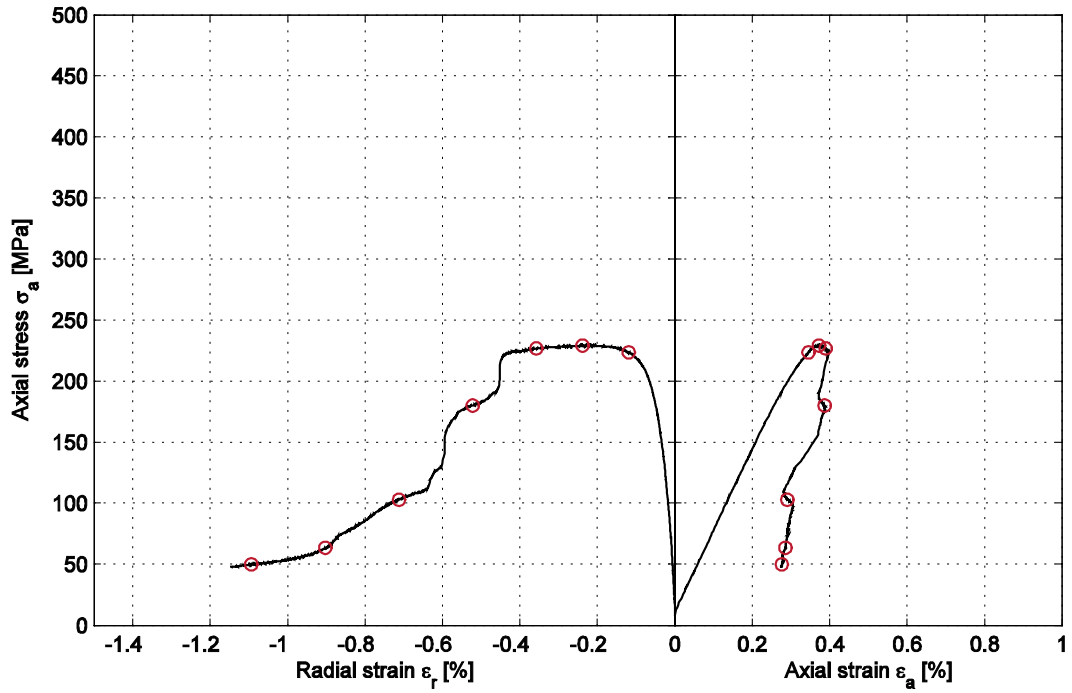
Specimen ID: KLX03A-115-08

Youngs Modulus (E): 66.5 [GPa]

Cell pressure: 7 [MPa]

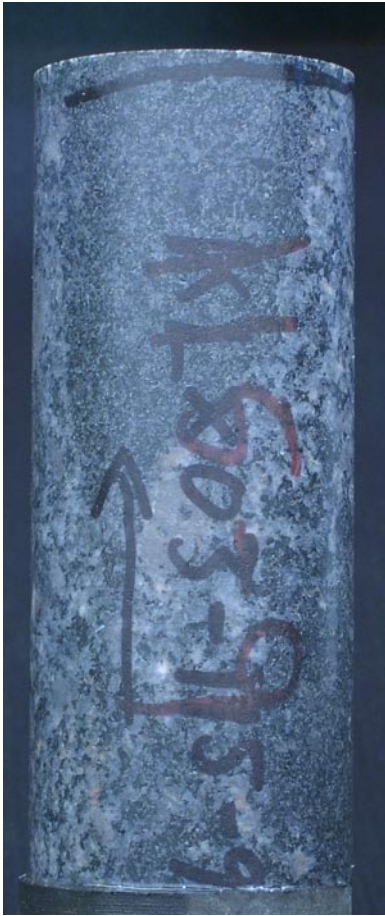
Poisson Ratio (ν): 0.199 [-]

Axial peak stress (σ_c): 229.1 [MPa]



Specimen ID: KLX03A-115-9

Before mechanical test



After mechanical test



Diameter (mm)	Height (mm)	Density (kg/m³)
50.2	125.2	2,800

Comments Diagonal shear failure. A sudden cracking in the post-failure region caused a large radial deformation, whereupon the system responded with a complete unloading.

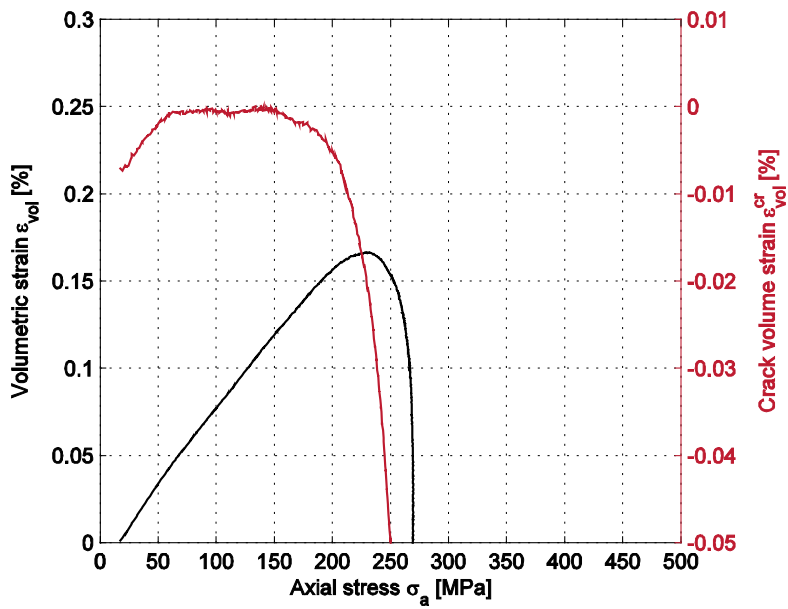
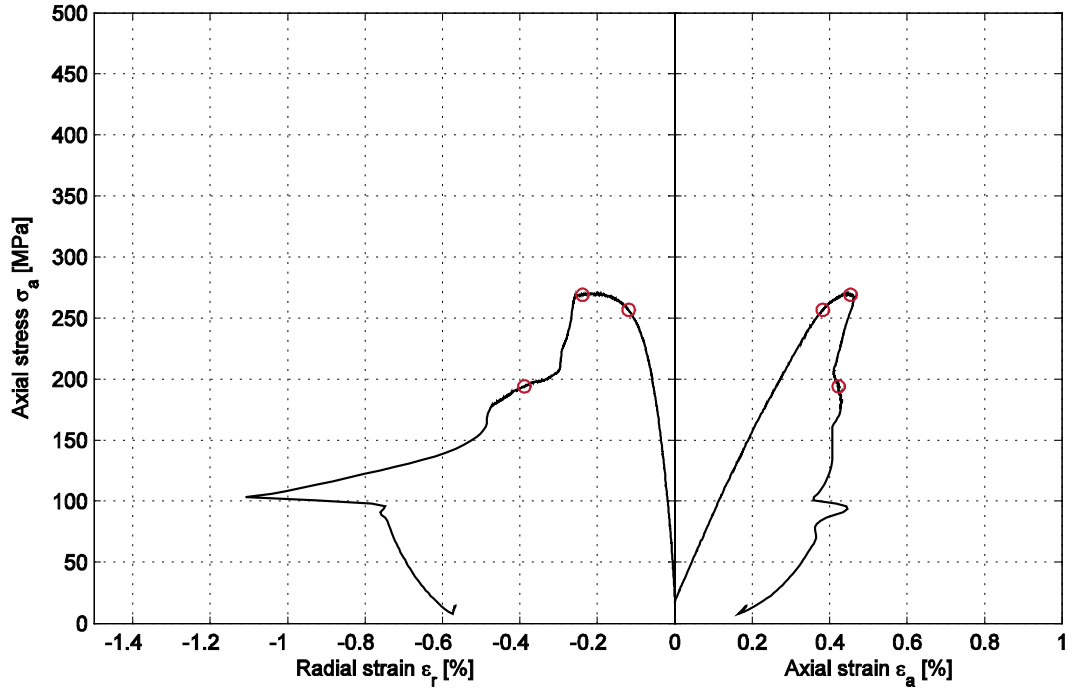
Specimen ID: KLX03A-115-09

Youngs Modulus (E): 65.3 [GPa]

Cell pressure: 15 [MPa]

Poisson Ratio (ν): 0.226 [-]

Axial peak stress (σ_c): 269.9 [MPa]



Specimen ID: KLX03A-115-11

Before mechanical test



After mechanical test



Diameter (mm)	Height (mm)	Density (kg/m³)
50.2	127.2	2,810

Comments Steep diagonal main failure and crack development in weakness planes of sealed cracks.

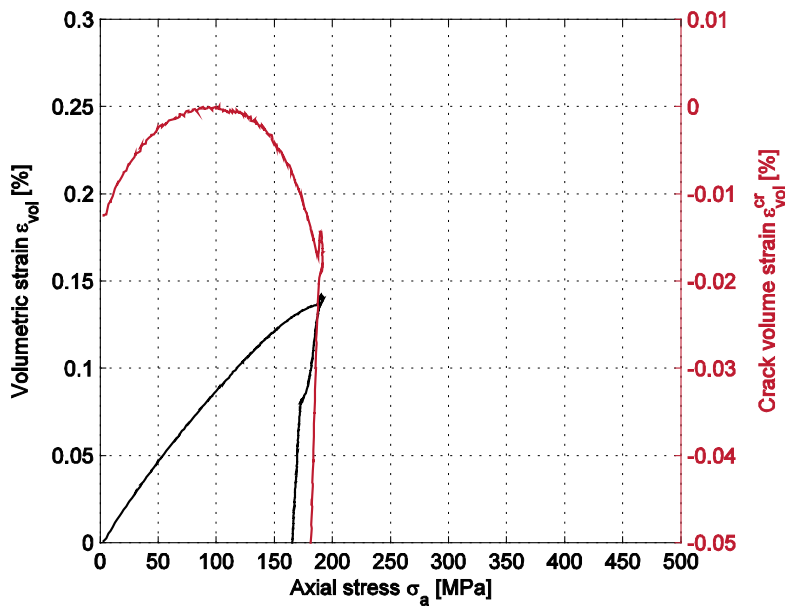
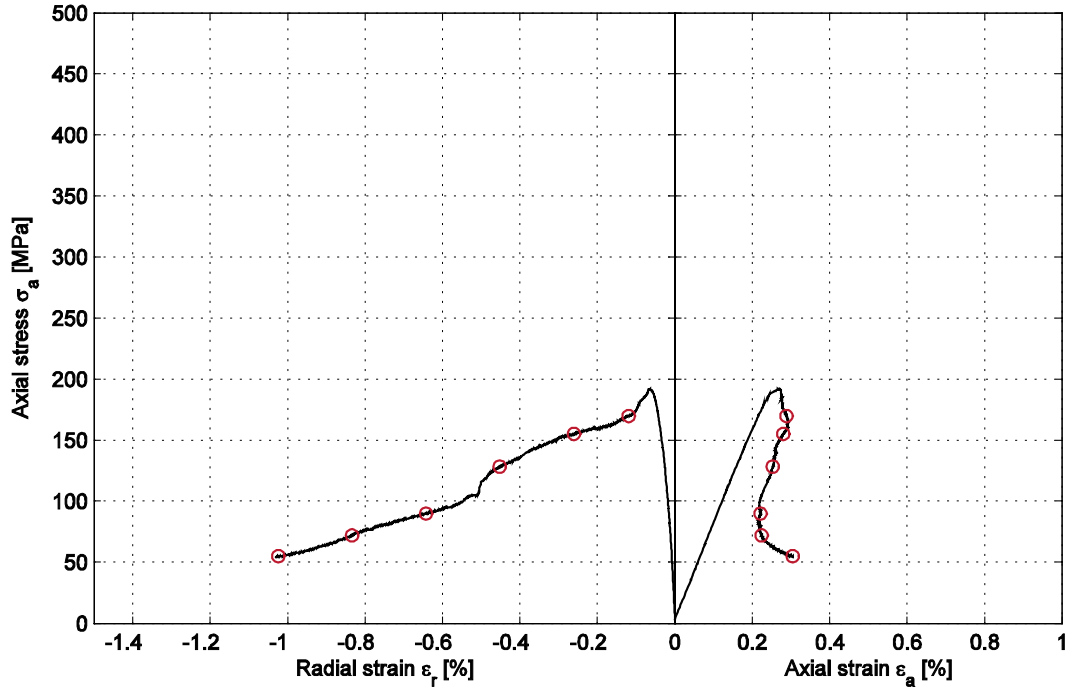
Specimen ID: KLX03A-115-11

Youngs Modulus (E): 79 [GPa]

Cell pressure: 2 [MPa]

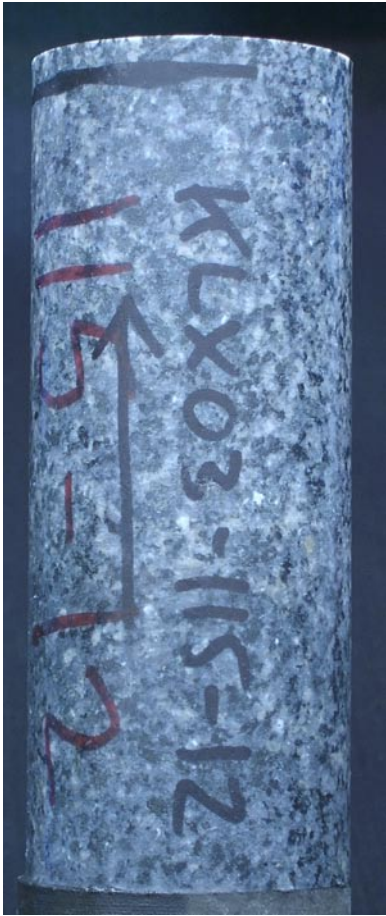
Poisson Ratio (ν): 0.199 [-]

Axial peak stress (σ_c): 192 [MPa]



Specimen ID: KLX03A-115-12

Before mechanical test



After mechanical test

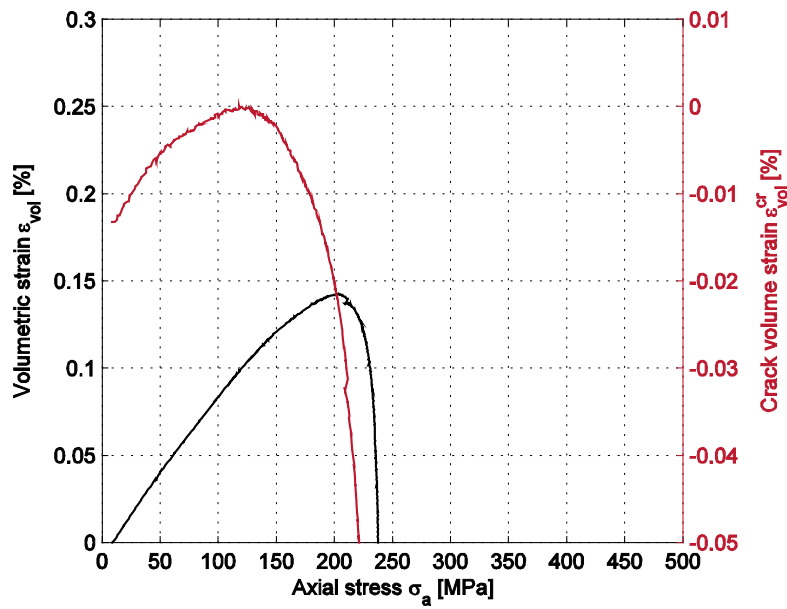
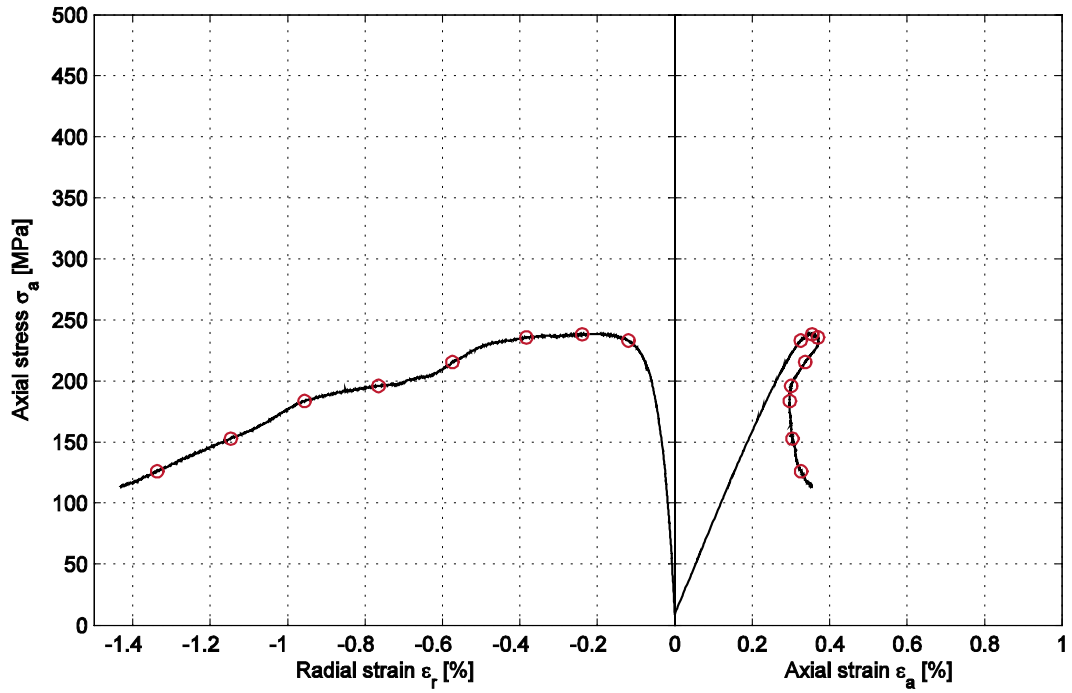


Diameter (mm)	Height (mm)	Density (kg/m³)
50.2	127.2	2,820

Comments Diagonal shear failure.

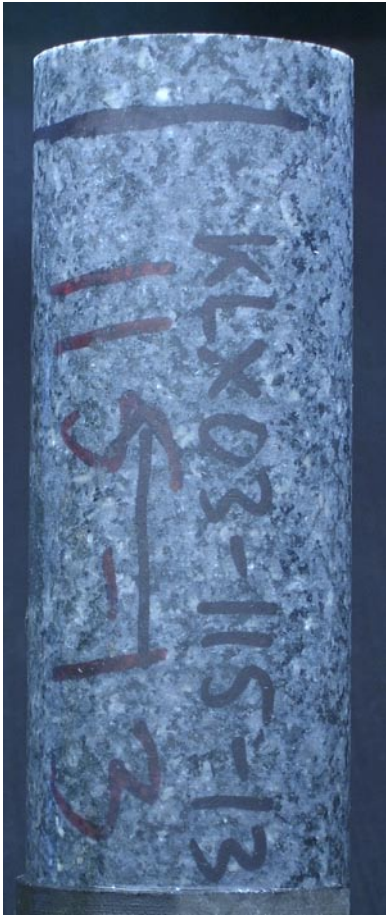
Specimen ID: KLX03A-115-12

Youngs Modulus (E): 74 [GPa] Cell pressure: 7 [MPa]
Poisson Ratio (ν): 0.212 [-]
Axial peak stress (σ_c): 238.6 [MPa]



Specimen ID: KLX03A-115-13

Before mechanical test



After mechanical test



Diameter (mm)	Height (mm)	Density (kg/m³)
50.1	127.4	2,810

Comments Steep diagonal failure.

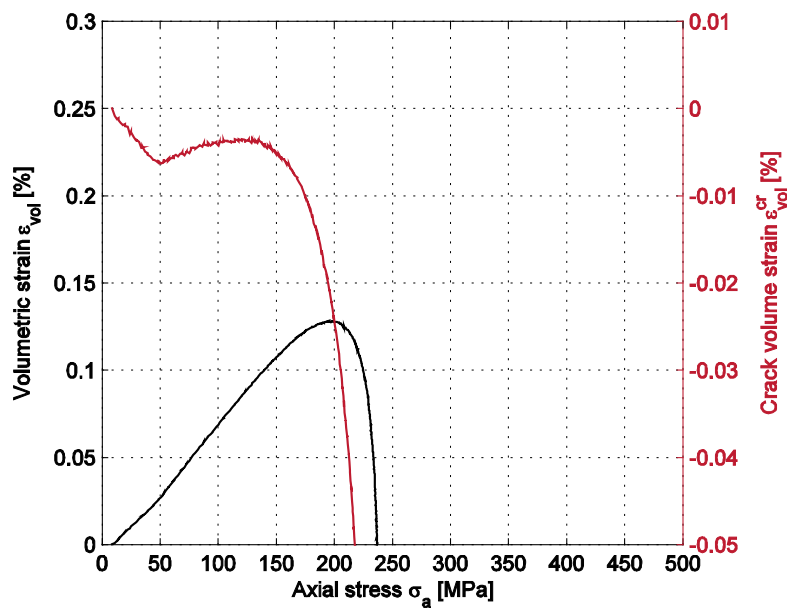
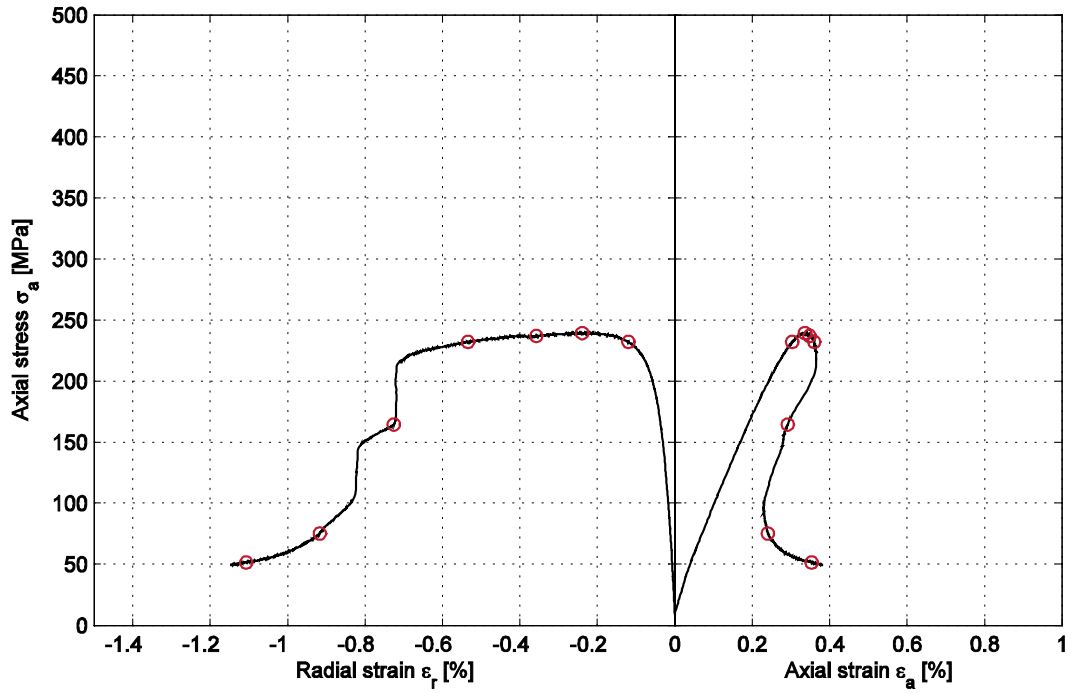
Specimen ID: KLX03A-115-13

Youngs Modulus (E): 75.6 [GPa]

Cell pressure: 7 [MPa]

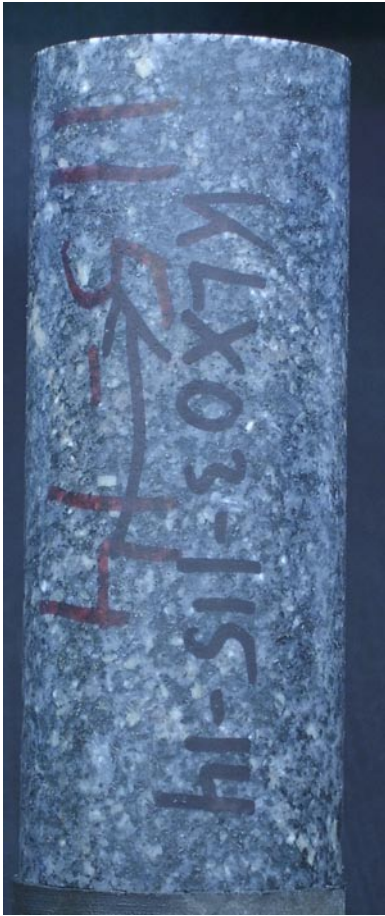
Poisson Ratio (ν): 0.2 [-]

Axial peak stress (σ_c): 239.3 [MPa]



Specimen ID: KLX03A-115-14

Before mechanical test



After mechanical test



Diameter (mm)	Height (mm)	Density (kg/m³)
50.0	127.7	2,790

Comments Diagonal shear failure. The membrane was punctured.

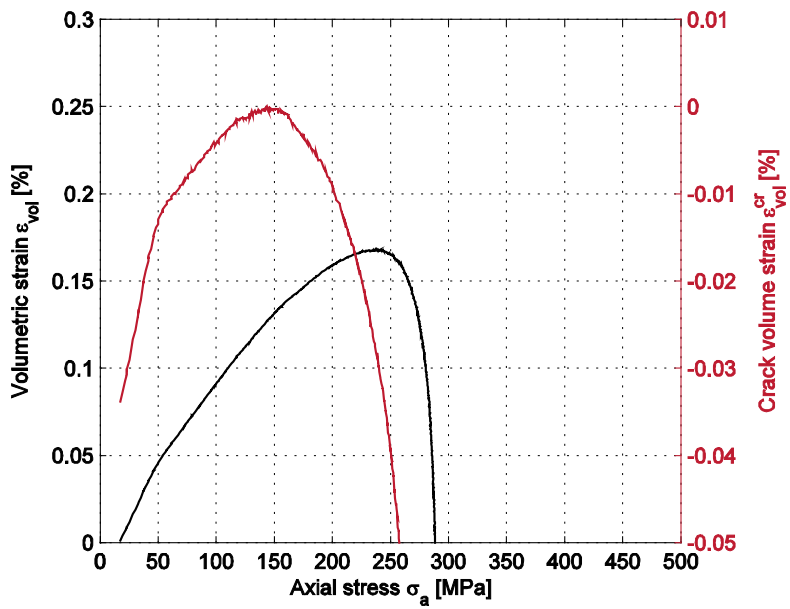
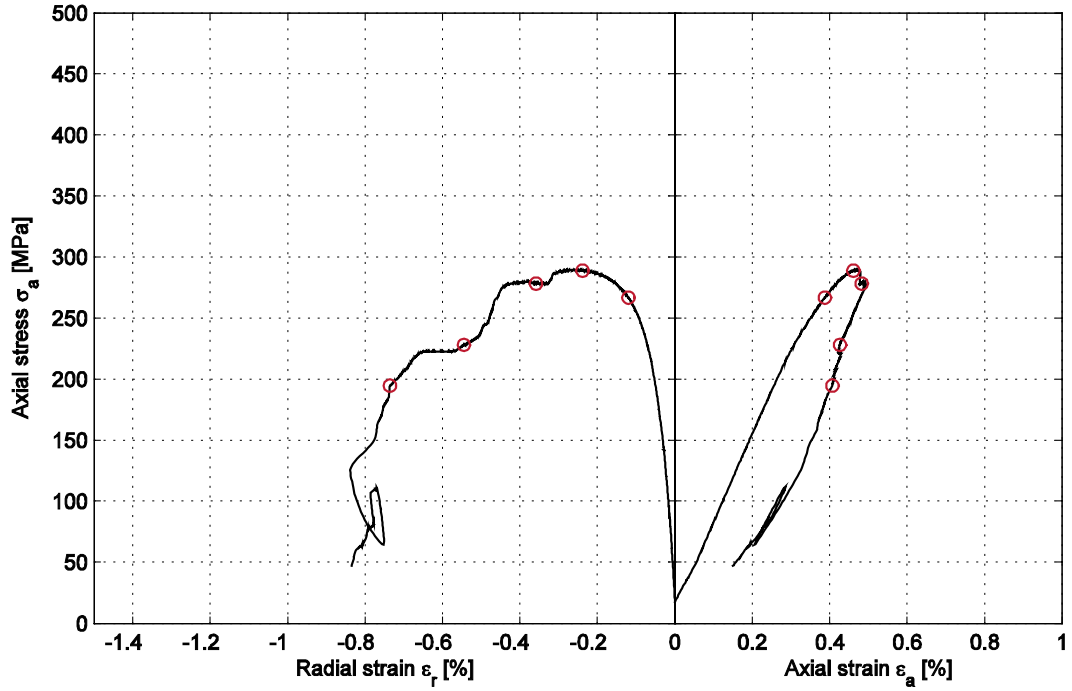
Specimen ID: KLX03A-115-14

Youngs Modulus (E): 71.8 [GPa]

Cell pressure: 15 [MPa]

Poisson Ratio (ν): 0.238 [-]

Axial peak stress (σ_c): 289.5 [MPa]



5.2 Results for the entire test series

A summary of the test results is shown in Tables 5-1 and 5-2. The densities, triaxial compressive strength, the tangent Young's modulus and the tangent Poisson ratio versus sampling depth are shown in Figures 5-1 to 5-4.

5.3 Discussion

The testing was conducted according to the method description except for one deviation. The circumferential strains have been determined within a relative error of 1.5%, which is larger than what is specified in the ISRM-standard /1/.

The activity plan was followed with no departures except for that specimen KLX03A-115-2 was replaced by specimen KLX03A-115-5 as data for the depth position in the drill hole was missing.

Table 5-1. Summary of results.

Identification	Conf press (MPa)	Density (kg/m ³)	Compressive Strength (MPa)	Young's modulus (GPa)	Poisson ratio (-)	Comments
KLX03A-115-1	2	2,770	188.7	69.9	0.23	
KLX03A-115-3	7	2,770	200.9	67.0	0.20	
KLX03A-115-4	15	2,780	303.5	64.1	0.21	
KLX03A-115-5	7	2,770	244.0	73.0	0.22	
KLX03A-115-6	2	2,760	178.2	59.4	0.17	
KLX03A-115-7	7	2,780	226.5	61.4	0.19	
KLX03A-115-8	7	2,780	229.1	66.5	0.20	
KLX03A-115-9	15	2,800	269.9	65.3	0.23	
KLX03A-115-11	2	2,810	192.0	79.0	0.20	
KLX03A-115-12	7	2,820	238.6	74.0	0.21	
KLX03A-115-13	7	2,810	239.3	75.6	0.20	
KLX03A-115-14	15	2,790	289.5	71.8	0.24	

Table 5-2. Calculated mean values and standard deviation.

	Density (kg/m ³)	Young's modulus (GPa)	Poisson ratio (-)
Mean value	2,787	68.9	0.21
Standard deviation	19.2	6.0	0.02

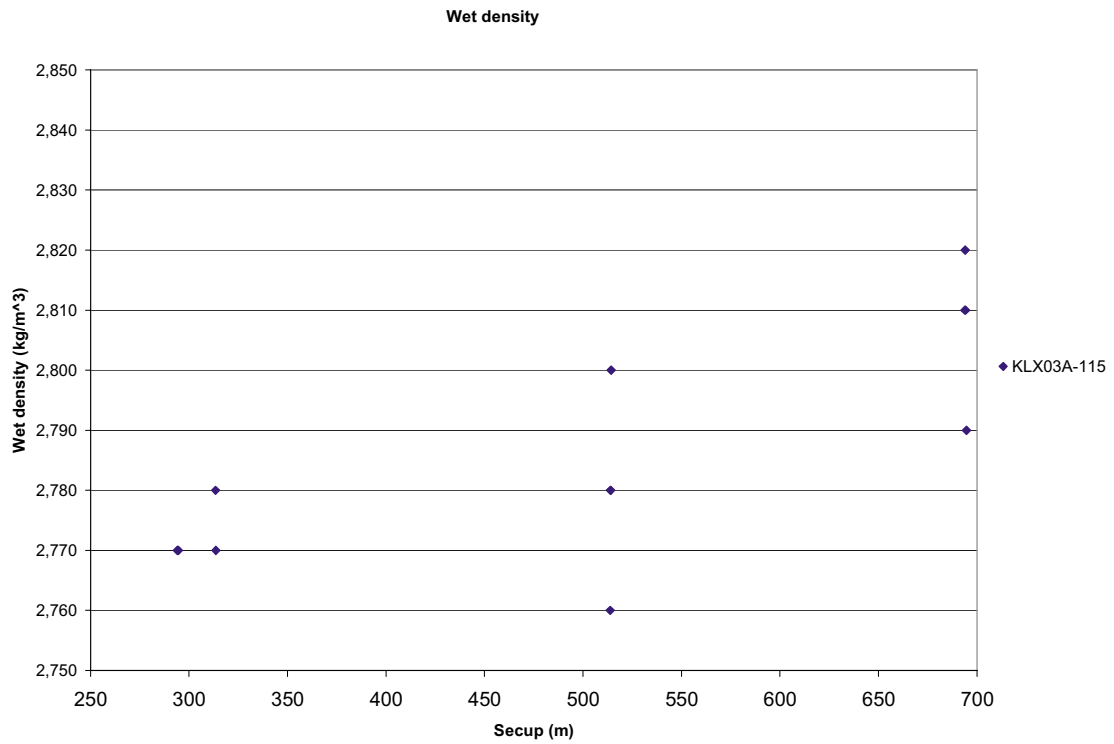


Figure 5-1. Density versus sampling depth in the borehole.

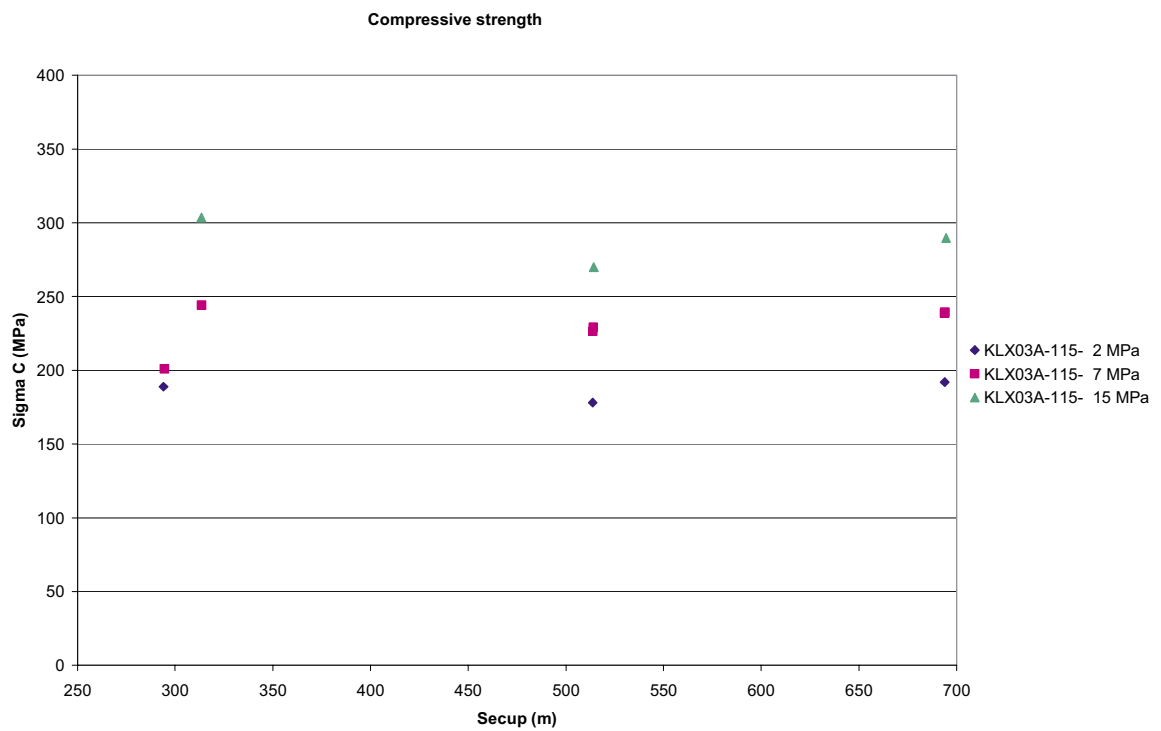


Figure 5-2. Compressive strength versus sampling depth in the borehole.

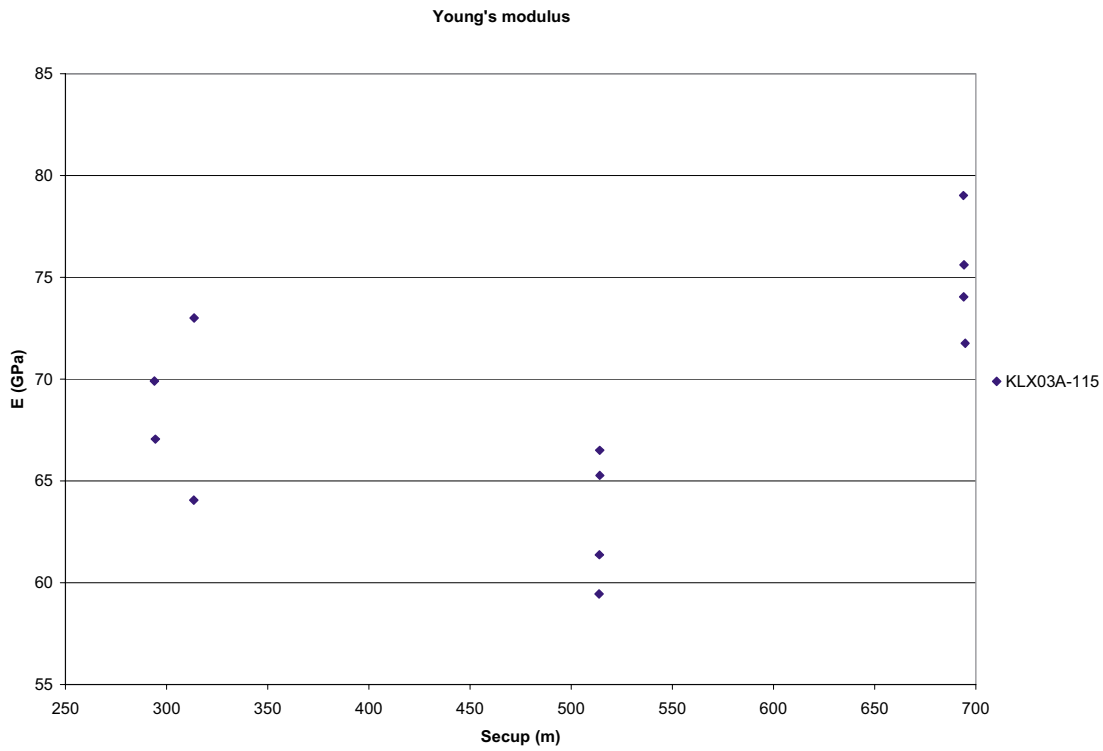


Figure 5-3. Tangent Young's modulus versus sampling depth in the borehole.

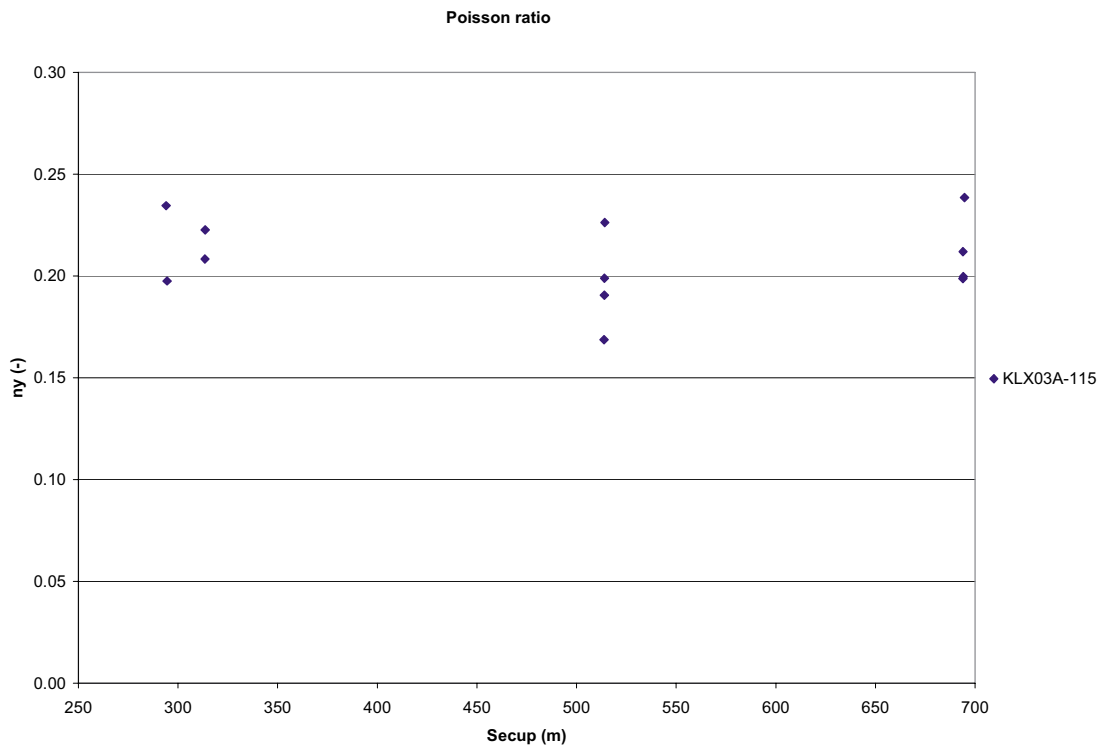


Figure 5-4. Tangent Poisson ratio versus sampling depth in the borehole.

References

- /1/ **ISRM, 1999.** Draft ISRM suggested method for the complete stress-strain curve for intact rock in uniaxial compression, *Int. J. Rock. Mech. Min. Sci.* 36(3), pp 279–289.
- /2/ **Martin C D, Chandler N A, 1994.** The progressive fracture of Luc du Bonnet granite. *Int. J. Rock. Mech. Min. Sci. & Geomech. Abstr.* 31(6), pp 643–659.
- /3/ **Eberhardt E, Stead D, Stimpson B, Read R S, 1998.** Identifying crack initiation and propagation thresholds in brittle rock. *Can. Geotech. J.* 35, pp 222–233.
- /4/ **ASTM 4543-01, 2001.** Standard practice for preparing rock core specimens and determining dimensional and shape tolerance.
- /5/ **ISRM, 1979.** Suggested Method for Determining Water Content, Porosity, Density, Absorption and Related Properties and Swelling and Slake-durability Index Properties. *Int. J. Rock. Mech. Min. Sci. & Geomech. Abstr.* 16(2), pp 141–156.
- /6/ **SS-EN 13755.** Natural stone test methods – Determination of water absorption at atmospheric pressure.
- /7/ **ISRM, 1983.** Suggested method for determining the strength of rock material in triaxial compression: Revised version, *Int. J. Rock. Mech. Min. Sci. & Geomech. Abstr.* 20(6), pp 283–290.
- /8/ **Stråhle A, 2001.** Definition och beskrivning av parametrar för geologisk, geofysisk och bergmekanisk kartering av berg, SKB-01-19. Svensk kärnbränslehantering AB. In Swedish.
- /9/ **MATLAB, 2002.** The Language of Technical computing. Version 6.5. MathWorks Inc.

Appendix A

The following equations describe the calculation of radial strains when using a circumferential deformation device, see Figure A-1.

$$\varepsilon_r = \frac{\Delta C}{C_i}$$

where

$C_i = 2 \pi R_i$ = initial specimen circumference

$$\Delta C = \text{change in specimen circumference} = \frac{\pi \cdot \Delta X}{\sin\left(\frac{\theta_i}{2}\right) + \left(\pi - \frac{\theta_i}{2}\right) \cos\left(\frac{\theta_i}{2}\right)}$$

and

ΔX = change in LVDT reading = $X_i - X_f$

(X_i = initial chain gap; X_f = current chain gap)

$$\theta_i = \text{initial chord angle} = 2 \pi - \frac{L_c}{R_i + r}$$

L_c = chain length (measured from center of one end roller to center of other end roller)

r = roller radius

R_i = initial specimen radius

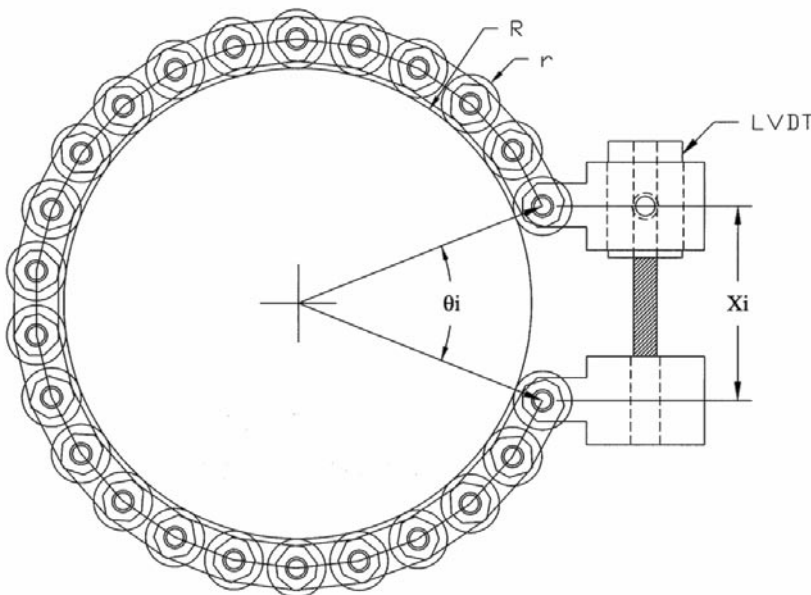
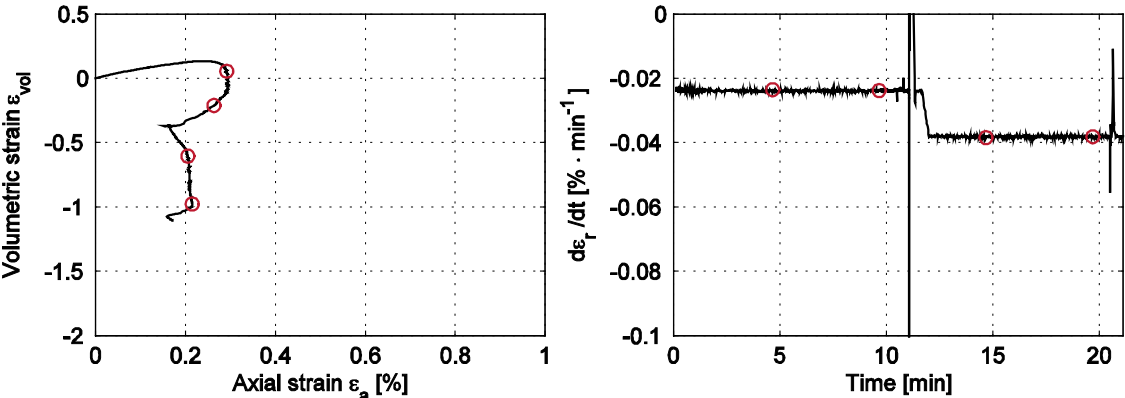


Figure A-1. Chain for radial deformation measurement.

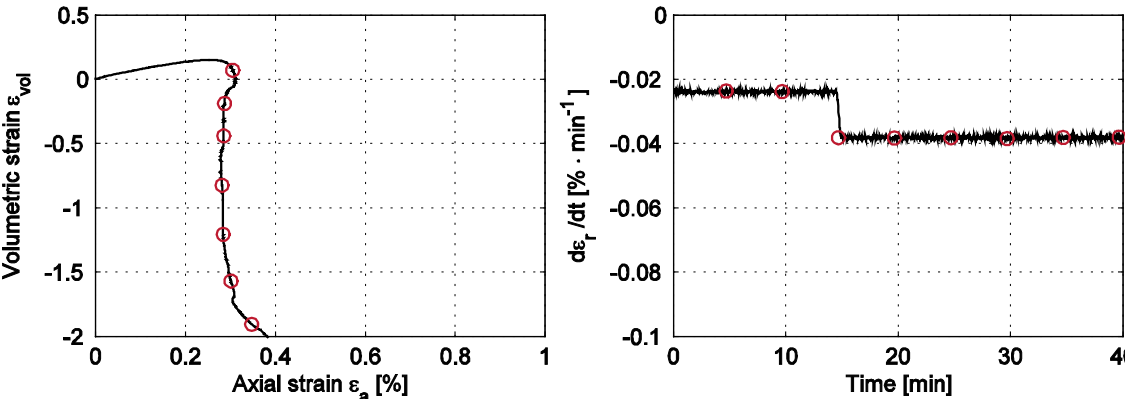
Appendix B

This Appendix contains complementary results showing the volumetric strain ϵ_{vol} versus the axial strain ϵ_a and the actual radial strain rate $d\epsilon_r/dt$ versus time. The complementary results for all tests are shown below.

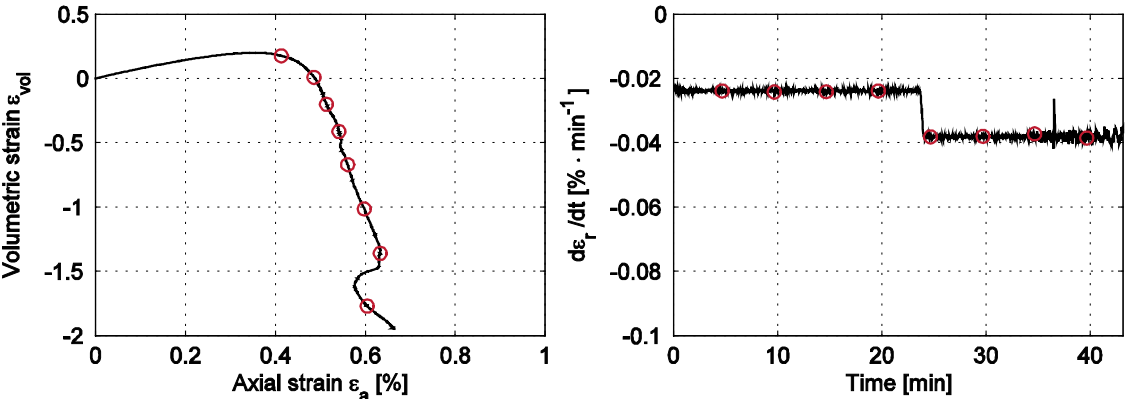
Specimen ID: KLX03A-115-01



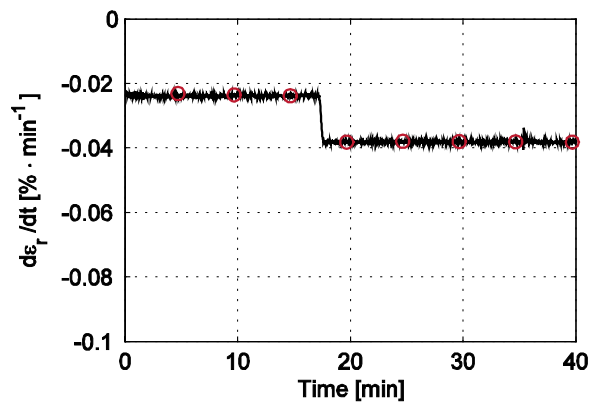
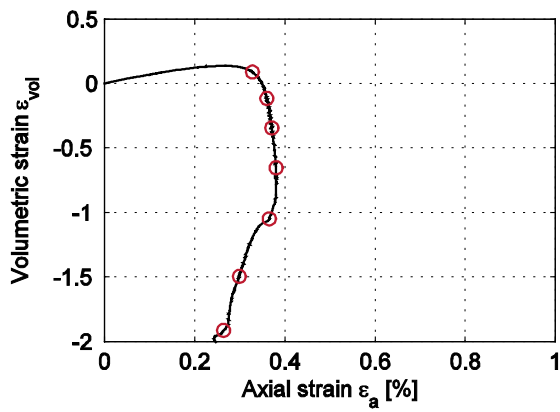
Specimen ID: KLX03A-115-03



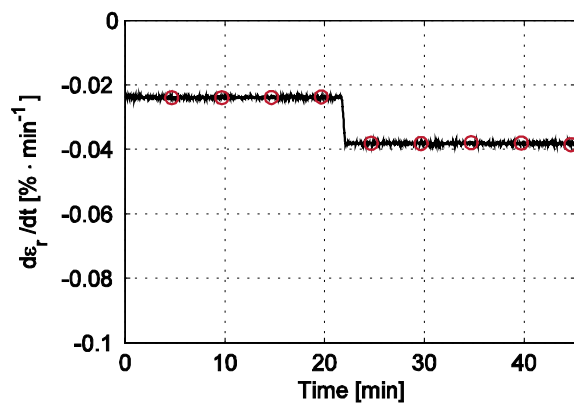
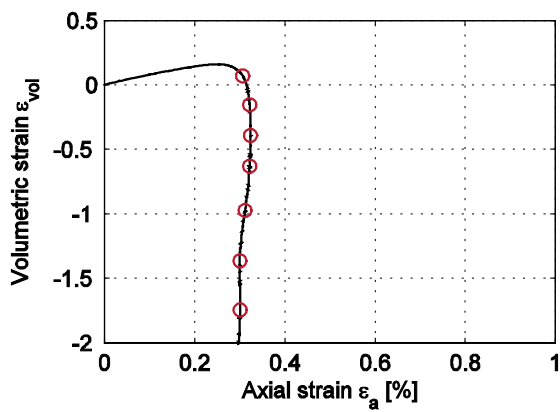
Specimen ID: KLX03A-115-04



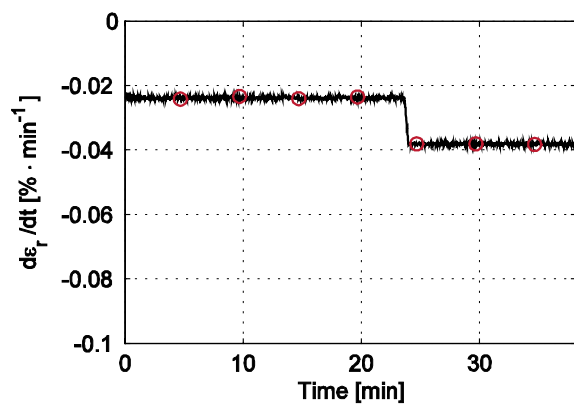
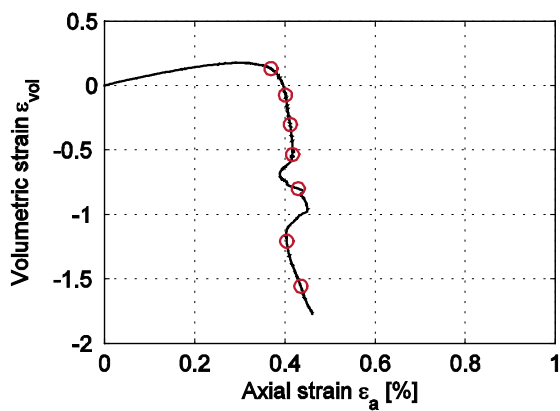
Specimen ID: KLX03A-115-05



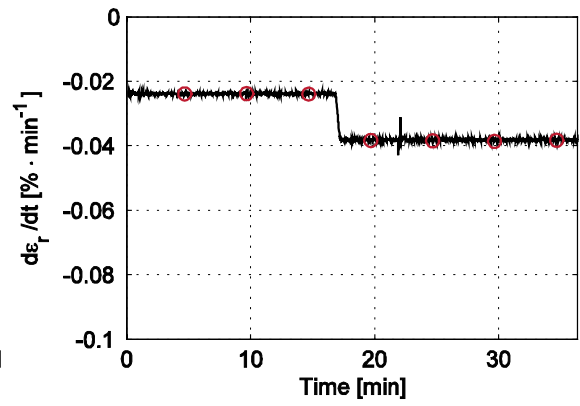
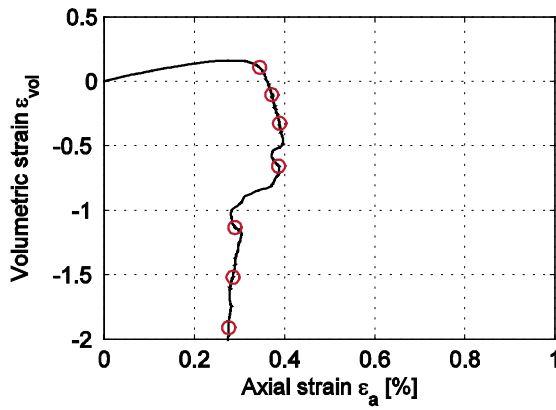
Specimen ID: KLX03A-115-06



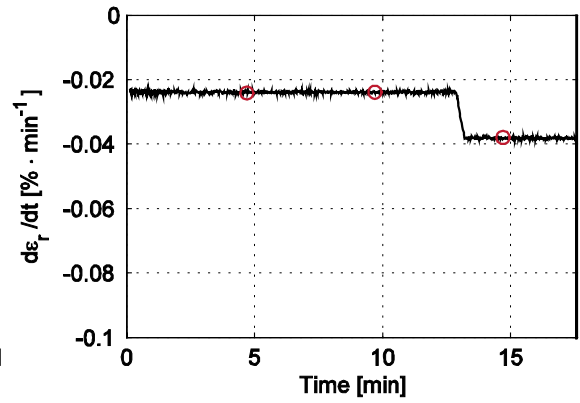
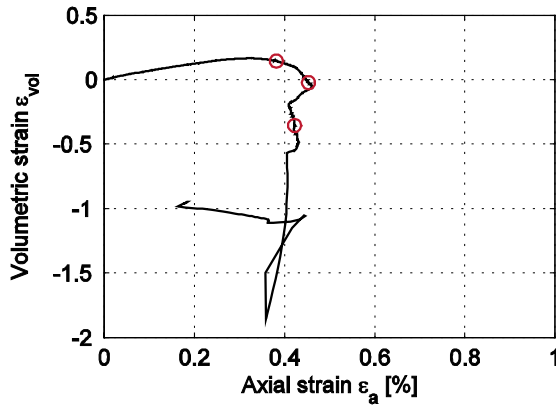
Specimen ID: KLX03A-115-07



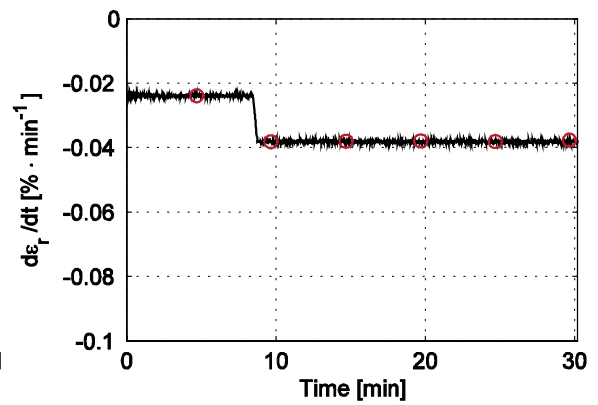
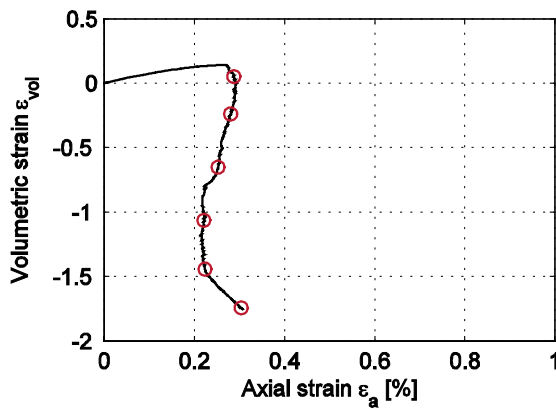
Specimen ID: KLX03A-115-08



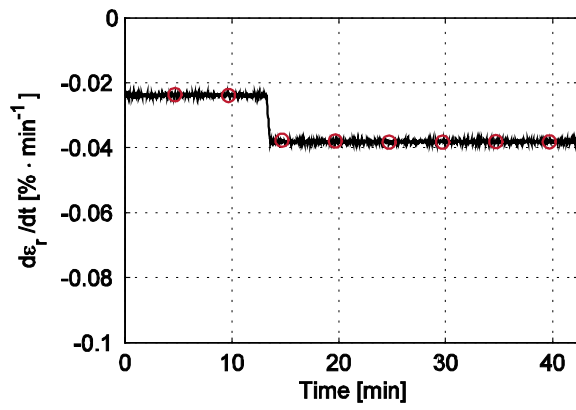
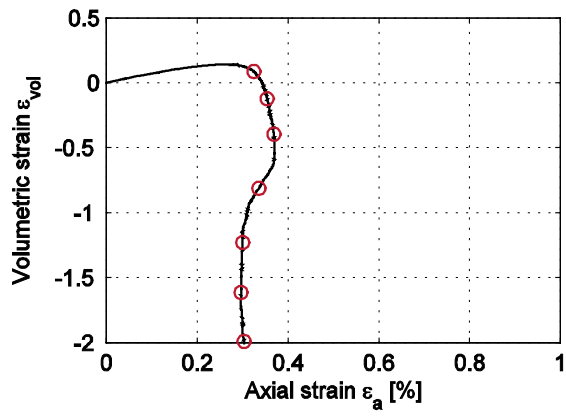
Specimen ID: KLX03A-115-09



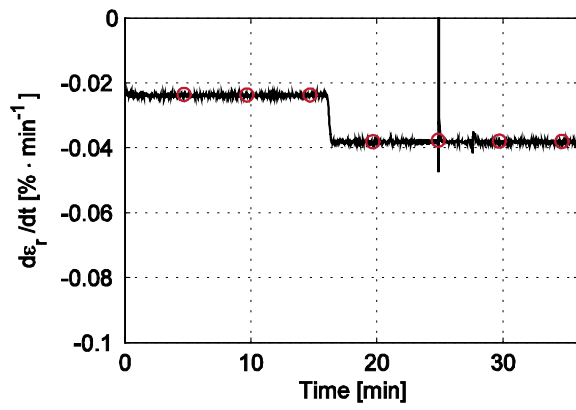
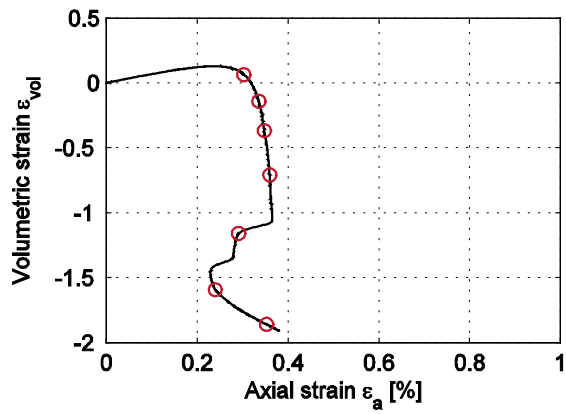
Specimen ID: KLX03A-115-11



Specimen ID: KLX03A-115-12



Specimen ID: KLX03A-115-13



Specimen ID: KLX03A-115-14

